

Sofie Barmen Stein

DC insulation materials for a modular HVDC generator

Electric stress testing of epoxy with and without silica filler

Master's thesis in Energy and Environmental Engineering

Supervisor: Pål Keim Olsen

Co-supervisor: Frank Mauseth

June 2022

Sofie Barmen Stein

DC insulation materials for a modular HVDC generator

Electric stress testing of epoxy with and without silica filler

Master's thesis in Energy and Environmental Engineering
Supervisor: Pål Keim Olsen
Co-supervisor: Frank Mauseh
June 2022

Norwegian University of Science and Technology
Faculty of Information Technology and Electrical Engineering
Department of Electric Power Engineering

Preface

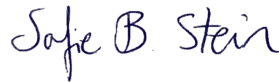
This work concludes my five-year journey at the Norwegian university of science and technology (NTNU). This master thesis is a part of the FME NorthWind project and focuses on the electrical insulation system of a modular HVDC machine, ModHVDC. The thesis was written on behalf of the Department of Electrical Power Engineering and completed in the spring of 2022.

I had not been able to complete this work without the help of others. I want to show my gratitude to my supervisor Pål Keim Olsen for his excellent guidance and engagement throughout the year. My co-supervisor Frank Mauseth also deserves my acknowledgment for his excellent advice and interesting input. I have highly enjoyed the biweekly meetings together with you.

I also thank Hans Helmer Sæternes for his guidance and availability in the casting lab. I greatly appreciate the time you set aside for me. In addition, a big thanks to Amar Abideen for always helping me and answering all my stupid questions. Your pep talks in a stressful period made me a little less stressed.

Last, but not least, a big thank you to the friends I have made over the years at NTNU. I am looking forward to new challenges in working life.

Trondheim, 07.06.2022



Sofie Barmen Stein

Abstract

A modular HVDC generator (ModHVDC) has been developed to meet offshore wind energy production challenges. It introduces a segmentation in the stator by dividing it into different modules and offer higher reliability, reduction of components, and DC at its terminals, making it desirable for an evolving HVDC transmission network. However, the entire design of the machine is not completed and is still in research. A challenge regarding the machine is the insulation system due to a DC potential in the stator, making it more complex than an AC insulation system. No suitable DC insulation materials have yet been developed for the modular machine.

This thesis investigates the modular HVDC machine's electrical DC insulation system design. Electric stress testing was performed on epoxy cups with and without silica filler to obtain lifetime curves. Due to DC complexity and the capacitive field when turning on/off the machine, AC was applied.

The work includes an introduction to the DC challenges when designing an insulation system for an HVDC machine. An approach to obtaining lifetime curves is also described. Further are a discussion concerning the design of test objects presented. Partial discharge tests were conducted at room temperature to verify the casting process of the test objects. An average breakdown voltage was found in breakdown tests at room temperature and 70 °C. The average BD voltage at 70 °C gave the basis in the accelerated aging tests were the applied voltage was decreased, and the time to breakdown was monitored.

The epoxy cups with and without silica fillers possessed different withstand strengths. At room temperature, the epoxy cups without silica fillers experienced the greatest average breakdown voltage of 41.6 kV compared to 31.9 kV in the epoxy cups with silica fillers. However, at 70 °C, no significant difference in average breakdown voltage was observed between the cups. The average breakdown voltage in the epoxy cups without silica fillers decreased by 16.5%, whereas no decrease was spotted in the epoxy cups with silica fillers. The epoxy cups with silica fillers withstood the temperature increase better than the epoxy cups without silica flour.

Several challenges took place regarding the accelerated aging tests. Working experimentally, many unforeseen obstacles occurred, and the master thesis time span was limited. The desired lifetime curves were not able to be obtained. Continuity of this work is needed, and several important aspects that need further investigation are introduced.

Sammendrag

En modulær HVDC-generator (ModHVDC) er utviklet for å møte utfordringene knyttet til produksjon av vindkraft til havs. Den introduserer en segmentering i statoren ved å dele den inn i forskjellige moduler og tilbyr høyere pålitelighet, reduksjon av komponenter og DC ved terminalene, noe som gjør den ønskelig for et HVDC-overføringsnettverk. Hele designet av maskinen er imidlertid ikke fullført og er fortsatt under forskning. En utfordring angående maskinen er isolasjonssystemet på grunn av et DC-potensial i statoren, noe som gjør det mer komplekst enn et AC-isolasjonssystem. Det er ennå ikke utviklet egnede DC-isolasjonsmaterialer for den modulære maskinen.

Denne oppgaven undersøker den modulære HVDC-maskinens elektriske DC-isolasjonssystemdesign. Elektrisk stresstesting ble utført på epoksykopper med og uten silica-filler med ønske om å oppnå levetidskurver. På grunn av DC-kompleksitet og det kapasitive feltet når maskinen slås på/av, ble AC brukt.

Arbeidet inkluderer en introduksjon til DC-utfordringer knyttet til det å designe et isolasjonssystem for en HVDC-maskin. En tilnærming for å oppnå levetidskurver er også beskrevet. Videre er en diskusjon angående design av testobjekter presentert. Partielle utladningstester ble utført ved romtemperatur for å verifisere støpeprosessen til testobjektene. En gjennomsnittlig gjennomslagsspenning ble funnet i gjennomslagstester ved romtemperatur og 70 °C. Den gjennomsnittlige gjennomslagsspenningen ved 70 °C ga grunnlaget i akselererte aldringstester der den påførte spenningen ble redusert, og tiden til gjennomslag ble målt.

Epoksykoppene med og uten silica-filler hadde forskjellige motstandsstyrker mot gjennomslag. Ved romtemperatur opplevde epoksykoppene uten silica-filler den største gjennomsnittlige gjennomslagsspenningen på 41,6 kV sammenlignet med 31,9 kV i epoksykoppene med silica-filler. Ved 70 °C ble det imidlertid ikke observert noen merkbar forskjell i gjennomsnittlig gjennomslagsspenning mellom koppene. Den gjennomsnittlige gjennomslagsspenningen i epoksykoppene uten silica-filler sank med 16,5%, mens det ikke ble observert noen nedgang i epoksykoppene med silica-filler. Gjennomslagsstyrken til epoksykoppene med silica-filler taklet økt temperatur bedre sammenlignet med epoksykoppene uten silica-filler.

Flere utfordringer fant sted under de akselererte aldringstestene. Ved å jobbe eksperimentelt oppsto mange uforutsette hindringer, og masteroppgavens tidsrom var begrenset. Levetidskurver ble ikke utviklet. Det er behov for kontinuitet i dette arbeidet, og flere viktige aspekter som bør undersøkes videre blir introdusert.

Disclaimer

As this thesis is a continuation of some of the work made in the specialization project in autumn 2021, reuse of literature is found.

Chapter 1, the introduction, has parts developed from the specialization project. More precise is the motivation, 1.1, the background information about the modular HVDC generator, 1.2, and the overview of the insulation challenges regarding the modular HVDC machine, 1.3, obtained from the specialization project. Some theory, in chapter 2, was written in the specialization project. This regards the first paragraph in 2.1 and the description of the Paschen law in 2.2.2. [1]

List of abbreviations

AC	Alternating Current
DC	Direct Current
HVDC	High Voltage Direct Current
ModHVDC	Modular HVDC machine
PD	Partial Discharge
PDIV	Partial Discharge Inception Voltage
PRPDA	Phase Resolved Partial Discharge Analysis
BD	Breakdown
IEC	International Electrotechnical Commission
TEAM	Thermal, Electrical, Ambient and Mechanical
DAQ	Data Acquisition
NI	National Instruments

Table of contents

Preface	i
Abstract	ii
Sammendrag	iii
Disclaimer	iv
List of abbreviations	v
1 Introduction	1
1.1 Motivation	1
1.2 The modular HVDC generator	1
1.3 Overview of the insulation challenges regarding the modular HVDC machine	2
1.3.1 AC and DC insulation in rotating machines	2
1.3.2 DC insulation challenges	5
1.4 Aim and approach	7
1.5 Scope	8
1.6 Content of thesis	8
2 Electrical insulation: characteristics and aging	9
2.1 Electrical insulation	9
2.1.1 Epoxy resin	9
2.1.2 Silica flour	9
2.1.3 Micro- and nano-composites: Epoxy resin with and without silica filler	10
2.1.4 Homogeneous and inhomogeneous electric fields	10
2.2 Aging of an insulation material	11
2.2.1 Thermal stress	12
2.2.2 Electrical stress	12
3 Modelling aging processes in electrical insulation materials	14
3.1 Design of an insulation system for a modular HVDC generator	14
3.2 Modelling	14
3.2.1 Lifetime curves for insulation	14
3.2.2 Collection of lifetime curve data	15
4 Experimental setup and test objects	17
4.1 Casting of test objects	17
4.2 Test approach on test objects	18
4.2.1 Partial discharge test	18
4.2.2 Breakdown test	20
4.2.3 Accelerated life aging test	20
4.3 Experimental setup	21
4.3.1 Testing at room temperature	21
4.3.2 Testing at 70 °C	25
5 Test results and discussion	27
5.1 Partial discharge test	27
5.1.1 Epoxy cups without silica filler	27
5.1.2 Epoxy cups with silica filler	28

5.1.3	Summary of discussion regarding PD results	29
5.2	Breakdown test	30
5.3	Accelerated aging test	32
5.4	Sources of error	33
6	Conclusion	34
7	Experience and further work	35
	References	38
	Appendix A Epoxy casting in cup configuration - approach	A-1
	Appendix B Epoxy with silica filler casting in cup configuration - approach	B-7
	Appendix C Examination of test objects before testing	C-8
C.1	Epoxy cups without silica filler: Casting A	C-9
C.2	Epoxy cups without silica filler: Casting B	C-10
C.3	Epoxy cups without silica filler: Casting C	C-10
C.4	Epoxy cups without silica filler: Casting D	C-12
C.5	Epoxy cups with silica filler: Casting A	C-12
C.6	Epoxy cups with silica filler: Casting B	C-13

1 Introduction

To reach the Paris Agreement and the goal to decelerate the global temperature on earth and not exceed the 2 °C threshold, a reduction in greenhouse emissions is crucial. All countries, especially industrial countries, are responsible for adjusting their consumption in a more clean and renewable way [2].

Numerous possibilities arise when forcing governments to develop low-carbon energy production. Wind energy technologies have drastically increased in scope in the past decades, estimating it will take a leading role in the restructuring of a renewable society [3]. Offshore wind farms are favorable compared to onshore wind farms as the sea consists of vast area resources.

The challenges for offshore wind farms span from installing floating wind turbines and reliability to costs. Another important aspect is the location from shore, which will affect the cable infrastructure [4]. By situating the wind farms far from shore, the significant distance will produce reactive losses in the AC cables, and the efficiency will go down. A solution to this problem is using DC cables. However, even though DC cables are cheaper than AC cables, the industry must install massive, expensive converter stations to meet the AC output from the wind turbines.

The installations of HVDC will likely expand in the future due to several planned HVDC lines [5]. Today, wind turbines deliver AC. However, a new generator, ModHVDC, is developed for offshore wind with a DC output [6]. The installation consists of a modular stator structure making the nacelle lighter. As it generates DC, the need for converter stations will be eliminated as well as the transformers, leading to higher efficiency at a lower cost. In addition, it will push the use of DC cables. Nevertheless, the machine also poses several challenges, especially in the electric insulation.

1.1 Motivation

Offshore wind could become Norway's new big technology marked. In 2020, the Norwegian government made it possible to apply for licenses to develop offshore wind farms in proposed sites [7]. In May 2022, the Norwegian government proposed expanding offshore wind production by 30 GW until 2040 [8]. With a further continuity in the evolving wind technology, offshore wind energy could be a promising industry, and solutions like the modular HVDC machine can become competitive. [1]

1.2 The modular HVDC generator

Before presenting the aim and approach, this section will introduce some background information about the modular HVDC generator.

The modular HVDC generator, ModHVDC, is a permanent magnet machine with concentrated windings. It has been developed to meet the challenges that arise with the constantly evolving technology and opportunities in the electrical infrastructure. Offshore wind is the primary intended application for this machine. However, growth within other power productions is also possible [9].

Offshore turbines have limited space, and the components inside the nacelle must not be too heavy. With the ModHVDC design, the help of power electronics can remove the transformer in the nacelle [6]. The machine is a modular machine, meaning that the stator is divided into segments. This segmentation gives air gaps between each segment, which is not typical for a non-modular machine. The stator core consists of thin iron lamination connected together. This lamination has sharp edges, which could lead to field enhancements. In the machine, each segment has a converter attached to it. Due to this, several components can be neglected, presented in Figure 1.1.

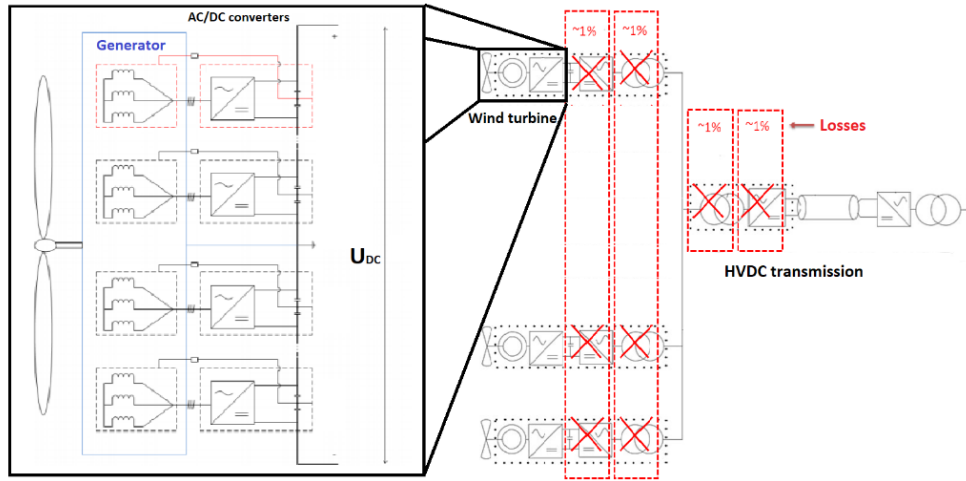


Figure 1.1: The ModHVDC concept with the reduction of components [10].

By being a segmented machine, maintenance is less challenging as each segment is independent, making bypassing possible [10]. Another advantage is that the reliability is increased due to the bypassing, as the machine will continue to work even though a malfunction in one of the segments occur [6].

As seen in Figure 1.1, the stator is floating on a DC potential given by the converters. The converters are connected in series, leading to different voltage potentials at each segment. Hence the machine output could be 100 kV or even higher [11].

For high voltage machines, insulation tends to be a big part of the machine weight [12]. The ModHVDC machine has a galvanic separation such that the AC and DC voltage are isolated, making it possible to have thinner insulation as the stresses are better distributed [13]. The insulation will, in addition, not be stressed in the same matter as a non-modular machine due to the segmentation, as the producing voltage is divided between the segments [6].

How HVDC affects an insulation system for electrical machines is not highly researched. Hence, further investigations are needed before a complete insulation system is developed for the modular HVDC machine. However, as the next chapter will present, DC is a complicated matter.

1.3 Overview of the insulation challenges regarding the modular HVDC machine

The modular HVDC generator poses several new challenges regarding DC insulation at high voltage stresses. Electrical insulation in rotating machines is a complicated matter. Hence, a clarification of the issue regarding the insulation system in the modular HVDC generator is needed.

1.3.1 AC and DC insulation in rotating machines

Both AC and DC will stress the stator in the modular HVDC generator. However, by a galvanic separation, they do not affect each other, making it possible to look at these two stresses apart from each other. Figure 1.2 shows the voltage stress distributions at one stator segment in a modular HVDC generator.

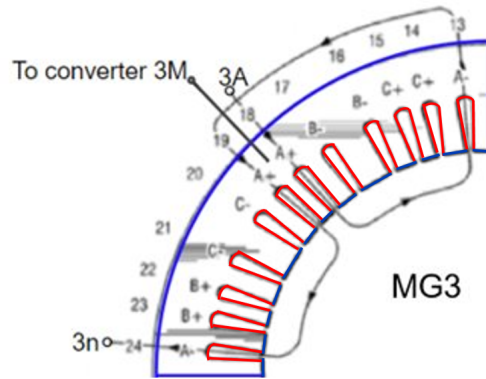


Figure 1.2: One segment of the stator in a modular HVDC generator [9]. The red marking is the winding area where AC occurs, while the blue marking is the area where the machine is stressed with a DC potential.

AC insulation

The AC in the modular HVDC generator acts on the stator slots, seen in Figure 1.2. Several levels of AC insulation are used in rotating machines. These are strand, turn and main insulation, shown in Figure 1.3 [14].

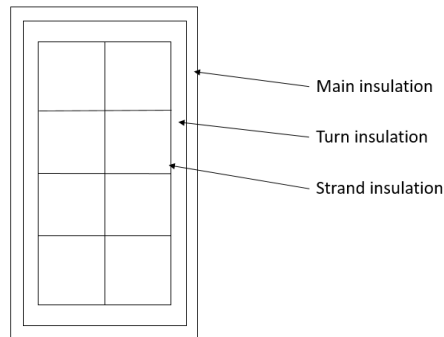


Figure 1.3: Overview of AC insulation in a winding structure with one winding [14].

The strand insulation isolates the conductors from each other and avoids unfortunate short circuits. The voltage over each strand is low, making the strand insulation thin. However, good thermal characteristics are critical as this insulation is closest to the conductors, where the highest temperatures will accumulate [14].

The turn insulation isolates the turns from each other as shown in Figure 1.4. This insulation is important as short circuits between turns can lead to high currents. It is also exposed to high temperatures due to its short distance to the conductors. Additionally, good mechanical properties are needed in turn insulation, as they are often bent when forming the winding structure in the machine. Vibration will also occur due to magnetically forces produced [14].

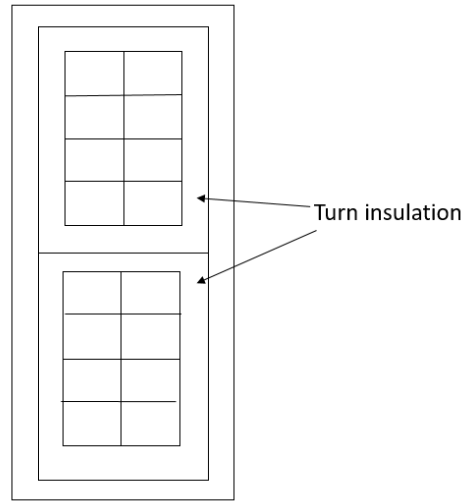


Figure 1.4: Turn insulation in a winding structure with two windings [14].

The outer insulation in the stator slots is the main insulation. This separates the stator from the conductors and is essential for heat dissipation. An excellent thermal conductivity is favorable for the main insulation. Due to the electrical fields created by the conductors, forces will act on the bar, making it vibrate. The main insulation also need to possess mechanical properties that can counteract these forces and the forces developed in each conductor [14].

DC insulation

The undertaking for the DC stator insulation, marked in blue in Figure 1.2, is to separate the stator from the machine housing (earth). Figure 1.5 illustrates the areas where the stator is stressed with DC, marked in blue. The DC insulation can be divided into segment-earth and segment-segment insulation. The segmentation is unique for the modular HVDC generator, giving air gaps between each segment. Another essential function of the insulation is hence to prevent discharges between each segment, as some air will circulate between them [9].

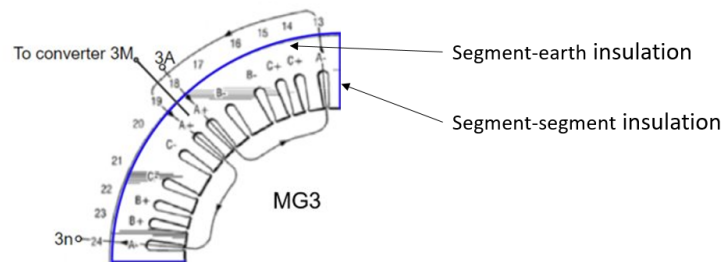


Figure 1.5: DC insulation in one segment of the stator in a modular HVDC generator, marked in blue [9].

1.3.2 DC insulation challenges

Other dilemmas occur when a machine is exposed to DC stress compared to AC stress. This will affect the electrical insulation in the modular HVDC generator. As AC has dominated high voltage machines for the last decades, the knowledge and experience of DC stresses are not highly developed. It is necessary to elucidate the main challenges and characteristics of DC stress on insulation.

DC development

DC behaves in the same manner as AC when switched on or off. A capacitive field is created, in the same way as AC, being decided by the permittivity ϵ . However, after some time, charges accumulate, making the DC system behave differently than AC. The field distribution develops into a resistive field controlled by the conductivity σ . Reaching stationary condition, a pure DC field will arise. However, even though a pure DC field can theoretically occur, it is not easy to obtain [15]. By switching off the voltage, surface charges start to disappear with a time constant [16].

Another vital aspect is when the polarity is switched. In the beginning, the capacitive field, in addition to the surface charges generated before, will remain in the material [16]. After some time, the surface charges will vanish, and new charges will form according to the new polarity. Reaching steady state, the pure DC field is achieved. However, it might not be the same as the former pure DC field as it has been discovered variations between the polarities [17] [16]. Figure 1.6 shows how the accumulation and dissipation of space charges occur.

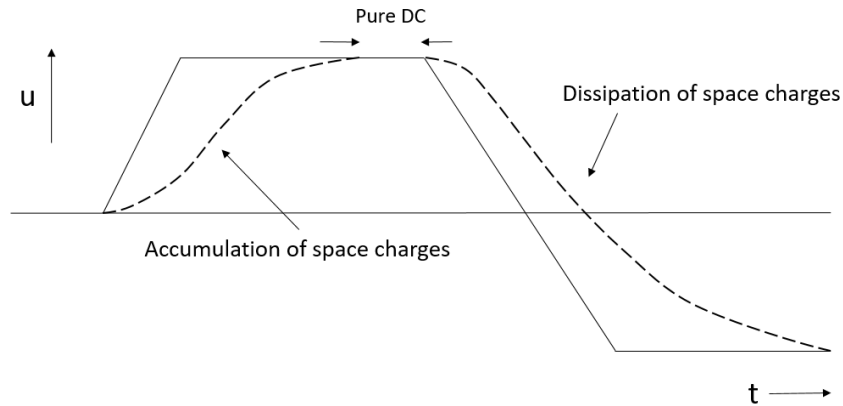


Figure 1.6: The development of DC as a function of applied voltage and time [16].

The conductivity is a sensitive parameter, and enough knowledge about it is not yet established [18]. Equation 1.1 shows the relation between the conductivity σ and the resistivity ρ of a material and how the conductivity increase exponentially with the temperature and electric field [16].

$$\sigma = \frac{1}{\rho} = \sigma_0 \cdot e^{\alpha T + \beta E} \quad (1.1)$$

σ_0 is the conductivity at 0 °C, α is the temperature dependency, and β is the electrical field dependency. Due to this correlation, the conductivity will face unpredictable properties when the temperature T and/or the electric field stress E increases. A high resistivity ρ is favorable for insulation materials. Hence a high conductivity due to a temperature and/or electrical field increase worsens the insulation material.

Electric stress: surface and space charges

Accumulation of charges occurs due to differences between charges flowing into a region compared to the charge flowing out of the same area. The relation can be expressed by the charge conservation equation, seen in Equation 1.2, developed by Maxwell's equations [18].

$$\frac{\partial \rho}{\partial t} + \nabla \cdot J = 0 \quad (1.2)$$

ρ is the charge density, and J is the electrical current density. Equation 1.2 explains how an increase in the current density correlates to a charge accumulation. The insulation material possesses ideal properties if no charge accumulation occurs. A low conductivity relates to a low amount of charge in the material. Charge accumulation is hence dependent on Equation 1.1.

Space charges occur above a specific field strength limit. By not exceeding this limit, the field will behave precisely like an AC field. With a further increase in temperature and electric field, space charges will start to accumulate [19].

The development of space charges can occur in several ways. The most common processes are homo and hetero charges, related to the cathode charge injection. Inadequate electron injection generates hetero charges at both electrodes, and the space charge polarities are equal to the electrodes. However, when too many electrons are sent through the material compared to what can be sent away, the space charge polarities will differ from the electrodes, and thereby homo charges occur. Hetero and homo charges are shown in Figure 1.7 [16].

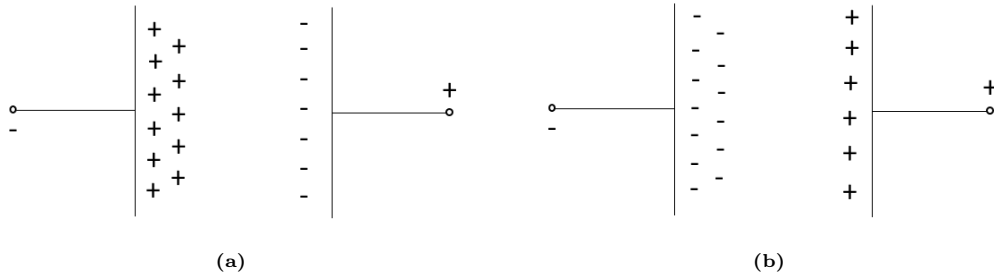


Figure 1.7: Space charge accumulation [16]: (a) Hetero charges; (b) Homo charges.

Homo and hetero charges affect the electric field as it either will be decreased or increased by the charge development [16], as seen in Figure 1.8. Hetero charges give an increased electric field close to the electrodes, while homo charges give a decrease.

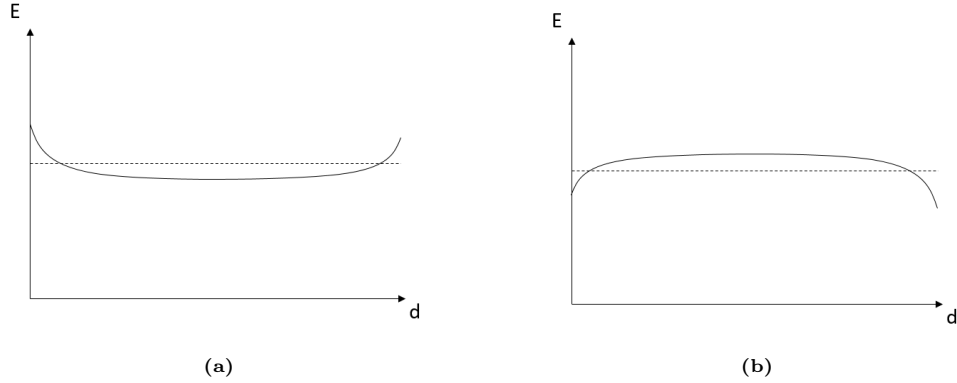


Figure 1.8: Field distribution [16]. The dashed line present the electric field without any charges: (a) Hetero charges; (b) Homo charges.

Surface charges typically develop at interfaces where the conductivity ρ and permittivity ϵ changes, as described by Equation 1.3 [16].

$$\rho = \nabla \cdot \left(\frac{\epsilon}{\sigma} \right) \quad (1.3)$$

Figure 1.9 shows a typical surface charge accumulation due to differences in interfaces [16].

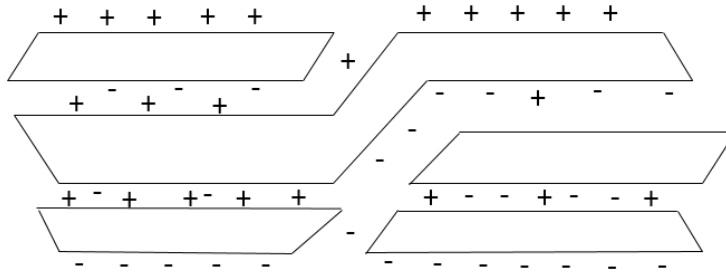


Figure 1.9: Surface charge accumulation where the interfaces changes [16].

Surface charges are expected for AC and DC systems. However, only space charges in DC systems make a noticeable impact. In addition, space charges are more difficult to measure than surface charges. This is why space charges are the main issues when dealing with DC [16].

1.4 Aim and approach

The main objective is to develop a DC insulation system design for the modular HVDC generator. Due to the complexity of DC stress on an insulation system and the presence of a capacitive electric field when turning on/off the machine, AC will be stressed on epoxy cups with and without silica filler, and lifetime curves will be from this established.

To obtain lifetime curves, several steps must be done beforehand. This thesis presents a discussion and approach regarding insulation design, casting procedure, partial discharge tests, breakdown tests and accelerated aging tests to acquire the desired database for lifetime curves.

1.5 Scope

This work was limited by several decisions and a short time span.

The insulation material used in the tests and in making lifetime curves was epoxy with and without silica filler. The silica filler was fused silica flour with micro-sized particles. 65 wt. % silica flour were used in the composite.

To simulate the machine's thermal operating state, testing was performed at two fixed temperature levels, at room temperature and 70 °C, where the latter represented the machine temperature best.

Electrical stress was regarded as the only aging contributor, known as single factor aging. The other TEAM stresses were not investigated.

The tests performed were stresses with AC.

1.6 Content of thesis

The master thesis consists of seven chapters. A short explanation of them is now presented.

- **Chapter 1:** The introduction consists of a presentation of offshore wind and the modular HVDC generator, in addition to an overview of the different insulation levels in rotating machines and the challenges in a HVDC insulation system. Motivation, aim and approach, and scope are also presented.
- **Chapter 2:** Literature review and essential theoretical aspects used.
- **Chapter 3:** Modeling and the data suggested to develop lifetime curves.
- **Chapter 4:** A description of the approach used to obtain the desired data. The development of the test object design and experimental setups for the different tests to be performed is described.
- **Chapter 5:** The results from the tests, in addition to discussion and comparison between the epoxy cups with and without silica filler. Last, sources of error are described.
- **Chapter 6:** Conclusion of the work done.
- **Chapter 7:** Description of experiences obtained from the work, in addition to suggested further work.

2 Electrical insulation: characteristics and aging

Relevant concepts related to the work will be reviewed in this section. First, electrical insulation and some typical materials used will be described. Afterwards, thermal and electrical stresses that affect the aging of an electrical insulation system are elaborated.

2.1 Electrical insulation

The main objective of an electrical insulation is to separate electrical objects with different potentials. For a machine designer, the insulation is troublesome as it is often the weakest point in a machine and does not produce any torque, only contributing to a more expensive design [20]. The consequence of poor insulation is current-flow in insulated areas, which could lead to degradation of the machine [21]. Another essential task for the insulation in a machine is to dissipate heat energy that accumulates. Having a good thermal conductivity and low dielectric losses are desirable for insulation [22].

The most obvious challenge for electrical insulation is electrical stress. However, thermal, mechanical, environmental and chemical stresses also highly affect the insulation and must be examined when developing a complete electrical insulation system.

Electric field grading is, from an insulation standpoint, crucial. It involves controlling the electric field in such a way that gives an acceptable electric field distribution [23]. Areas consisting of sharp edges and impurities pose a threat towards the electrical insulation due to the accumulation of high electric field [24]. These characteristics must be avoided when producing electrical insulation intended for rotating machines.

Epoxy resin is highly used in electrical machines as insulation material [25]. By introducing additives like fillers, powders, or other types of layers, manipulation of the epoxy is possible to achieve desired properties [26]. This manipulation could be favorable when developing an insulation design in a HVDC machine, as it introduces the possibility of custom design when no similar work has been done. In the following subsections, a short material characteristic of epoxy resin and a commonly used filler, silica flour, is presented. In addition, are some relations needed to be considered when designing and testing an electrical insulation system introduced.

2.1.1 Epoxy resin

Epoxy is a thermosetting resin that is a widely used insulator due to its excellent dielectric properties [27]. It has been utilized and known for decades, but still, it is highly evolving and improving today. Hence, thousand of different epoxy configurations exists today with different characteristics [28]. Typical applications where epoxy is utilized are in generator insulation and switchgears [24] [29].

A curing process is needed due to the thermosetting properties [24]. When curing, the epoxy resin goes from a fluid into a hard solid in a reaction known as cross-linking. Due to this cross-linking, properties desirable for high voltage insulation arise. A hardener is often used with an accelerator to begin the curing process. Their compositions also vary, giving numerous different epoxies [28]. As curing changes the chemical structure of the epoxy, they can not be recycled and remelted.

Shrinkage will occur in the resin due to the curing [30]. These mechanical stresses can cause cavities and impurities undesirable for an insulation material [28]. Due to shrinkage, the insulation might perform poorer, which is a challenge.

2.1.2 Silica flour

It is common to use composite materials for insulation to obtain desired characteristics. These consist of typical polymers with additives like fillers, powder, or other types of layers [26]. Silica dioxide (SiO_2) is a common filler used in composites, often known as silica flour or quartz powder.

Many different silica filler configurations exist, such as fused silica and crystalline. Crystalline silica is extracted from quartz while fused silica is melted and crushed crystalline silica. Fused silica has finer particles compared to crystalline silica and is hence easier to mix with an epoxy solution [31].

The weight percent (wt. %) of silica filler in composites can vary greatly. However, with the right amount, the desired characteristics in the electrical insulation can be improved, such as tensile strength, dielectric strength, and thermal conductivity [28]. An increased amount of filler loading over 40 % leads to a higher viscosity [32]. With high viscosity, the casting process will be more tedious. In addition, due to the increased viscosity, blending the filler is an important task, as poor blending could cause cavities in the compound.

2.1.3 Micro- and nano-composites: Epoxy resin with and without silica filler

The effect of adding fillers to a polymer is highly researched. The size of the silica particles play an essential part in the breakdown strength. By adding fillers, field concentration might form due to cavities made [29]. Research states that micro-sized silica particles do not necessarily improve the breakdown strength [33]. However, literature shows that by using nano-sized fillers, its breakdown strength exceeds the breakdown strength compared to the epoxy resin without fillers [34]. In [35], the breakdown strength of the epoxy resin filled with nano-sized silica is increased by 18 %. Hence, using silica at the nano-level might make a positive contribution to the dielectric properties [29].

In [33], epoxy resin with nano-sized silica filler with wt. % of 5 experienced a higher electric field strength than epoxy resin without the additive. These tests were performed at room temperature, and the test object was a needle-plate electrode configuration.

It must be addressed that by adding additives to a polymer, not only the electrical properties will be affected. Investigations show that both mechanical and thermal properties could be altered by the adding of silica fillers [36]. The totality of the properties must hence be monitored.

2.1.4 Homogeneous and inhomogeneous electric fields

An electrical insulation system in a homogeneous electric field experience an uniform electric field distribution. Areas with sharp edges like corners, impurities and interfaces often experience higher and non-uniform field concentrations. This is known as inhomogeneous electric fields [24].

Figure 2.1 illustrates the difference between homogeneous and inhomogeneous electric field distribution. The figures marked in grey is the electrodes, the yellow area demonstrates a solid electrical insulation, while the blue marking is a fluid. The arrows symbolize the electric field, where the middle area in the insulation has a homogeneous electric field, while inhomogeneous fields arise at the corners of the electrodes.

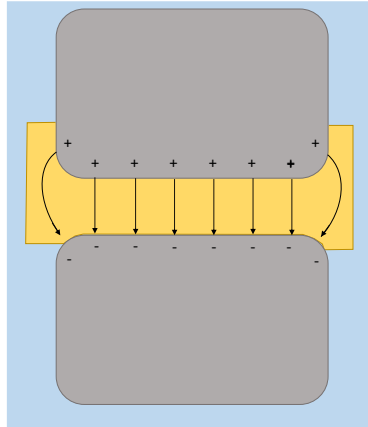


Figure 2.1: Illustration of homogeneous and inhomogeneous electric field distribution [24]. The grey areas are electrodes, the yellow area is a solid electrical insulation, while the blue color is a fluid. The black arrows show the direction of the electric field.

Making the field distribution homogeneous when designing an electrical insulation system is desirable. Inhomogeneous electric fields are far more challenging as field gradients easily arise in areas where the electric field does not follow a uniform distribution, making the insulation more vulnerable to discharges [24].

2.2 Aging of an insulation material

IEC 60505 defines aging as "irreversible changes of the properties of an electrical insulation system due to action by one or more stresses [37]." Aging happens due to the numerous stresses that cause aging processes in the electrical insulation [24]. It must be addressed that each stress often affects the other stresses.

A producer of an electrical insulation system must know the lifetime of its products. If a product is broken before the minimum lifetime set, the purchaser (or the producer) will suffer economic consequences. Thirty years is a normal life expectancy used when designing electrical components and insulation [24]. However, failure could occur sooner or later. Figure 2.2 present the well-known bath tube curve [38]. The probability of failure is highest at the start and end of the lifetime. Even though the aging of insulation material is inevitable, the goal when producing them is to expand their life as much as possible.

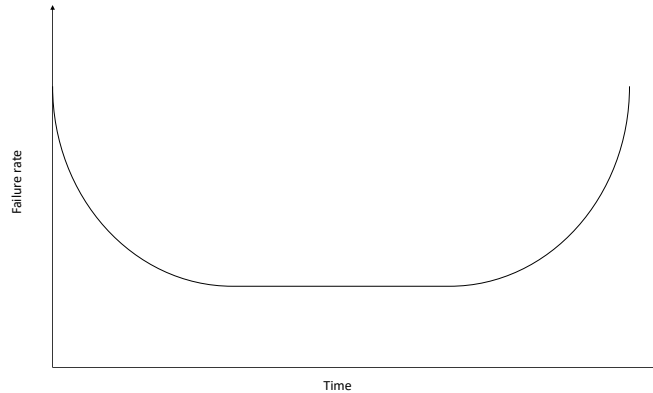


Figure 2.2: Bath tube curve illustrating the probability of failure in an insulation system over time [38].

Two of the most common type of stresses towards an insulation system, thermal and electrical stress, will now be presented.

2.2.1 Thermal stress

Thermal stress occurs with changes in temperatures. By an increased temperature, the insulation material could achieve unsuitable characteristics. If the heat generated is more significant than what the electrical insulation can dissipate, a thermal breakdown and development of hot spots can occur [24][39]. Other stresses could generate heat as dielectric losses or partial discharges. Another effect of increased thermal stress is an increased thermal expansion which could affect the mechanical stresses [40]. In addition, a thermal expansion of the insulation could lead to cavities, posing a threat towards the electric field strength.

An increase in temperature could affect the withstand strength of insulation material. Some literature has found a decrease in withstand strength with increased temperature [41]. However, this will be highly affected by the composition of the insulation material.

Thermal stress has a close relation to the electrical stresses, as increased electrical stress could increase the temperature and hence the thermal stresses [42].

2.2.2 Electrical stress

Electric stress can accelerate several aging processes such as partial discharges, water trees and electrical trees which eventually could lead to electric breakdown [23] [39]. Electrical stress is also highly dependent on the other stresses.

If water and an electric field are present, water trees might develop. They grow slowly, but they are especially troublesome as they reduce lifetime expectancy drastically [24]. Electrical trees are often initiated due to water trees, and eventually, the insulation is broken [43].

IEC 60270 defines partial discharge as: "localized electrical discharge that only partially bridges the insulation between conductors and which can or can not occur adjacent to a conductor [44]." Partial discharges occur in voids, and the Paschen curve can find the discharge voltage for air in a homogeneous field. The breakdown voltage changes by varying the gap distance d and/or the gas pressure p . The Paschen curve in Figure 2.3 shows how a decrease in the gap distance will lead to a decrease in breakdown voltage when the gas pressure is kept constant. However, the breakdown voltage will increase when the distance reaches a certain distance. This also applies to the gas pressure when the distance is kept constant. Thus, the breakdown voltage can be expressed by a function of the gas pressure and gap distance known as the Paschen law [24].

$$U = f(p, d) \tag{2.1}$$

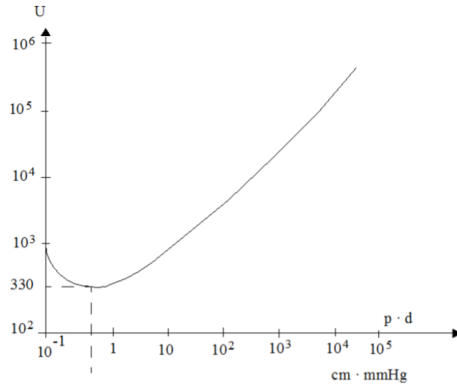


Figure 2.3: Paschen curve for air, obtained from [24].

Partial discharge (PD) and breakdown (BD) phenomena follows a stochastic distribution [45]. The discharge voltage level will vary when provoking PD or BD in an electrical insulation material repeatedly. Different statistical techniques can say something about the probability of PD and BD at given voltage values. However, no clear determination of PD or BD voltage of insulation can be made [24]. A way to minimize the uncertainty regarding the PD or BD voltage is by performing multiple PD or BD tests.

3 Modelling aging processes in electrical insulation materials

Several considerations must be evaluated when designing an insulation system. This section presents a discussion regarding the approach to obtaining lifetime curves.

3.1 Design of an insulation system for a modular HVDC generator

When designing an insulation system for a modular HVDC generator, data regarding the lifetime of the insulation system must be collected. Lifetime curves are tools to examine the lifetime of an insulation system. No research regarding the insulation system in the modular HVDC generator has yet been developed. Data must hence be established to be able to create a full-fledged insulation design for the machine.

The data should be representative of the operation state of the modular HVDC generator. The most interesting topic is how the DC stress will affect the insulation material. However, DC stresses pose several challenges, and uncertain data is likely to arise. Several good arguments can be made regarding doing the first developing of lifetime curves under AC stress. The DC insulation in the modular HVDC machine, seen in Figure 1.5, is exposed to a capacitive field, as seen in Figure 1.6, when turning on/off. It must hence withstand AC stresses as well. Whether a pure resistive field can be achieved under an operation state is also highly debated, as described in Section 1.3.2. Thus, developing AC lifetime curves will also give valuable input to the insulation system and final result.

3.2 Modelling

Before lifetime curves can be created, an overview of the data needed must be presented. This subsection introduces the modelling of lifetime curves.

3.2.1 Lifetime curves for insulation

Lifetime curves can be made for an electrical insulation system with the help of accelerating life aging test and extrapolation [24]. IEC 60505 suggests ways to find the lifetime of an electrical insulation system when changing the different TEAM (thermal, electrical, ambient, mechanical) stresses [37]. Changing more than one stress is possible, known as multi-factor aging. However, this is a complicated matter. A less challenging approach is to vary one of the stresses while the others are set to constant. This is known as single-factor aging.

Regarding the electrical stress aging, IEC 60505 suggests the inverse power law model when making lifetime curves, seen in Equation 3.1 [37]. This is the most used approach when examining electric stresses and is valid when the other aging factor is unchanged [46].

$$L(V) \propto xV^{-n} \tag{3.1}$$

L is the lifetime, V the applied voltage, and n the voltage life exponent [37][46]. Figure 3.1 shows an example of a typical lifetime curve with electric stress as aging factor [24].

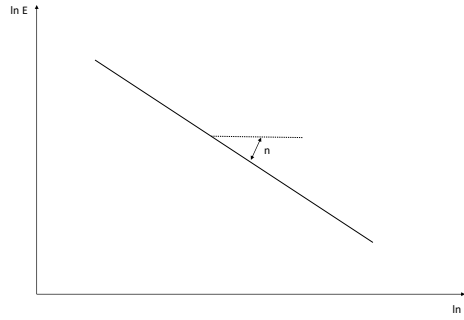


Figure 3.1: Lifetime curve with electric stress as aging factor, obtained from [24].

3.2.2 Collection of lifetime curve data

Several stresses affect the lifetime of an insulation system, as described in Section 2.2. It is hence these stresses the insulation material must be exposed to when data regarding its lifetime is to be obtained. Whether a single-factor or multi-factor aging is appropriate for the insulation system must be decided.

As mentioned in the scope, mechanical and environmental stresses will not be a part of this work. The modular HVDC machine will operate at a constant temperature and the thermal stresses are assumed to be steady. Due to this, electric stress will be used as a single-aging factor.

IEC 60505 proposes the inverse power model when modelling lifetime curves of an insulation system with electrical stresses as the single-aging factor, seen in Equation 3.1 [37]. This is also an highly acceptable model, considerably used in the literature [20][39][47][48][49][50]. The parameters in Equation 3.1 must be found to be able to develop lifetime curves.

From experiments, the applied voltage V and the time-to-breakdown L can be found with the help of accelerating aging tests. In [50], n was found to be between 9 and 12 for epoxy with a void at DC voltage. [24] say n is found to be between 8 and 14 in synthetic polymers. By assuming n , the constant x can be calculated.

As single-factor aging of the insulation material is conducted in this work, only electric stress is the accelerated part in the accelerated aging tests [48][37]. To obtain the starting values for the accelerated aging tests, breakdown (BD) tests must be performed [50]. Figure 3.2 shows how a lifetime curve can be made with the help of BD and accelerating aging tests [42]. When the BD voltage of the insulation material is found from the BD tests, the voltage level is decreased, and the time-to-breakdown is monitored in the accelerated aging tests. IEC 60505 suggests at least three different voltage levels when performing accelerated aging tests [37].

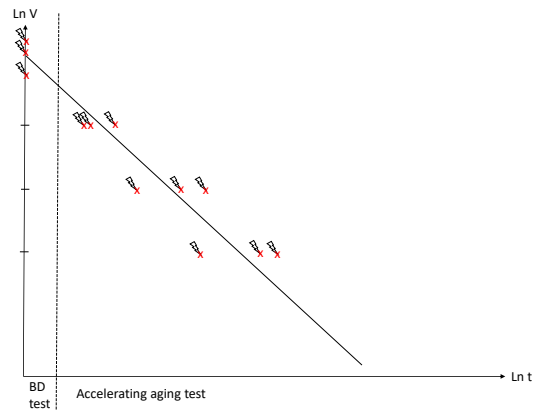


Figure 3.2: Principle of how to obtain a lifetime curve with the help of BD and accelerated aging tests as a function of time and voltage [42]. From the breakdowns (lightning) at different voltage levels, a linear graph can be drawn in a log-log representation of the axis, showing the life of an insulation system. This illustration has three tests at each voltage level.

4 Experimental setup and test objects

High voltage experiments must be performed to obtain the desired data described in Chapter 3. However, before the experiments can be conducted, the appearance of the test object must be decided. This chapter presents the steps towards the basis needed to obtain lifetime curves.

4.1 Casting of test objects

The chosen insulation material for the test objects is epoxy with and without silica filler. Epoxy is attractive due to the ability to manipulate its properties when adding fillers. Several shapes of the test object are relevant. A discussion regarding the most favorable design for the test objects will now be presented.

Several mold form configurations were considered. A needle-formed electrode with insulation material surrounding it, was discussed. This would have simulated the stator core lamination in the modular HVDC generator, described in Section 1.2. However, several challenges arise with this design. As numerous test objects must be made, their production must not be too time-consuming. No standardized mold form for this type of design was easily available. Hence, the production would have taken time as it would likely be done by casting the insulation material and then drilling a hole in it, inserting the needle electrode. In addition, would this likely lead to several errors as microscopic cracks in the interface. The design would also give an uncontrollable electric field, as the needle tip would provide a strong inhomogeneous electric field.

A rod-plane gap configuration was reviewed. The clear advantage of this design is the ability to examine a two-layered insulation system. An insulation system consisting of a solid insulation material and air would match the insulation system in the modular HVDC machine as air circulates between the segments, as described in Section 1.2. However, a two-layered insulation system is far more complex than a one-layered insulation system due to the interface between them, where charges are likely to accumulate.

As this is the first work regarding the insulation system for the modular HVDC generator, a mold form shaped like a cup was chosen. This was due to the favorable electric field distribution in this form, as only the rounded corners will experience an inhomogeneous electric field. In addition, were the cup mold forms easily available such that no notable time was used regarding making the design. The thickness of the bottom was set to 1 mm. Figure 4.1 and Figure 4.2 show the appearance of the cups produced. Two different types of cups were made, epoxy cups with and without silica filler. The same material relation is used for them except for the exclusion of silica flour for the epoxy cups without silica filler.

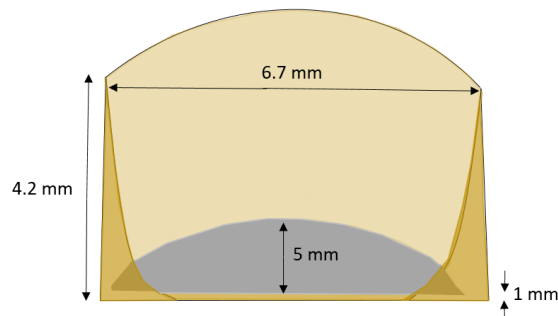


Figure 4.1: Sketch of cross-section of a cup with measurements. The grey bottom illustrates the semiconducting paint.



Figure 4.2: Cast cups: (a) Epoxy cup without silica filler; (b) Epoxy cup with silica filler.

The cups were made in a casting laboratory. Appendix A and Appendix B describe the approach used to produce the epoxy cups without silica filler and the epoxy cups with silica filler, respectively. Appendix C shows the examination of the cups under a microscope.

A conducting layer, CoronaShield P 8003, is painted on each cup to obtain good contact between each cup and the electrodes. To avoid field enhancement, the painting must be smooth, and no sharp edges should occur. The varnish should be painted around the corners of the bottom so that the inhomogeneous field areas do not become vulnerable to electric field stress. The epoxy cups without silica filler are transparent, making it easy to spot large impurities before applying the semiconducting tape. The epoxy cups with silica filler are grey, and it is hence harder to observe pollution in these cups visually and in a microscope. Figure 4.3 shows coated epoxy cups without silica filler.

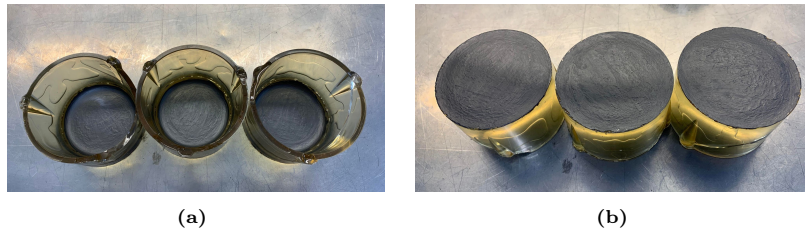


Figure 4.3: Coated epoxy cups without silica filler with CoronaShield P 8003.

Sources of error are likely to occur when preparing the insulation materials for testing. As the test object is not fabric-made, several obstacles, such as micro-dust, fat marks, or cavities, can interfere with the results. Any touching of the cups must be kept at a minimum.

4.2 Test approach on test objects

After the preparation and production of the test objects, the data needed to establish lifetime curves was found by performing breakdown (BD) and accelerated aging tests. In addition, was partial discharge (PD) tests conducted.

Before presenting the experimental setup for each test, an introduction to partial discharge, breakdown and accelerating aging tests is necessary.

4.2.1 Partial discharge test

The main objective of a partial discharge test is to monitor partial discharges when increasing the voltage over a test object. Such tests can tell if the insulation material contains voids which can later degrade the

insulation system and lead to a complete electric breakdown. This is highly used in the industry to quality check electrical insulation systems [44][51].

IEC 60270 proposes a conventional way to detect partial discharges. The electrical components and instruments needed for the measurements are also presented, in addition to the test setup [44].

A common way to observe PD propagation is by a Phase Resolved Partial Discharge Analysis (PRPDA). When examining PRPDA patterns, an understanding of what type of PD that occurs can be made. For instance, a typical characteristic when PDs happen in a void in PRPDA patterns are feather-like arrangement situated in each half period, creating a symmetric pattern. However, it must be addressed that the PRPDA is affected by multiple factors, and a complete conclusion can be challenging to obtain [51].

Partial discharge inception voltage (PDIV) is the voltage level where the first PDs is observed. When decreasing the voltage, PDs will still occur. However, eventually, the PDs will cease. This voltage level is known as the extinction voltage [51] [24].

The discharge magnitude that occurs under PD can not be measured. Hence, another charge is measured under PD testing, known as apparent charge. IEC 60270 defines apparent charge as "apparent charge of a PD pulse is that charge which, if injected within a very short time between the terminals of the test object is a specified test circuit, would give the same reading on the measuring instrument as the PD current pulse itself [44]." The ABC-model for electrical insulation with a cavity will now be further elaborated.

ABC-model

An ABC-model of an electrical insulation system, in addition to an external circuit, is used to explain how PDs can be measured [51].

The insulation can be divided into three sections of capacitance, seen in Figure 4.4. C_a represents the capacitance over the insulation, C_c represents the capacitance of the cavity and C_b represents the capacitance of the insulation in series with the cavity [24].

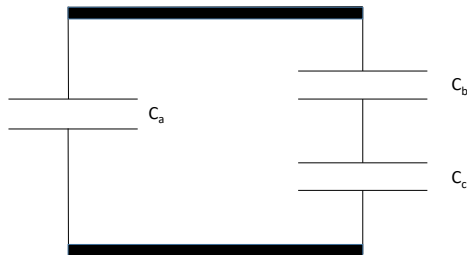


Figure 4.4: ABC-model [24][51].

With the help of the ABC-model and an external circuit, seen in Figure 4.5, partial discharges inside an insulation material can be detected [51].

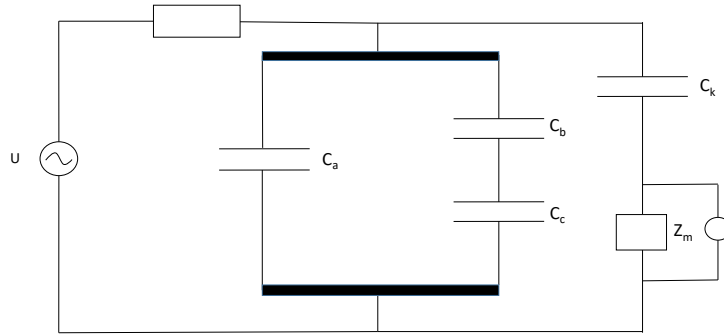


Figure 4.5: Test circuit for PD measurement consisting of the ABC-model and an external circuit [24][51].

When a partial discharge occurs in the cavity, a current will flow in the external circuit seen in Figure 4.5. The impedance Z_m , also known as a measuring impedance, can detect this current (apparent charge) and thereby say something about how large the discharge is. Due to the voltage drop in the cavity, voltage needs to be restored over the void. Hence a coupling capacitor, C_k , connected in parallel, could be used to supply the needed charge [51].

4.2.2 Breakdown test

An electrical breakdown in an insulation system occurs when the insulation is not able to withstand the electric field. When this happens, a conductive bridge develops in the insulation, possessing undesirable characteristics of an insulation system [24].

With a breakdown test, the withstand voltage for the electrical insulation system is found. However, it must be noted that by performing a breakdown test, the insulation system is turned into an irreversible state [24]. The applied voltage should be started at zero voltage and be ramped up until a breakdown in the electrical insulation system occur. The time duration at each voltage step must be such that the electric field gets enough time to stabilize [52].

The occurrence of breakdown follows a stochastic distribution. It is hence necessary to do numerous breakdown tests under the same condition to get a good understanding of the withstand strength of an electrical insulation system [24][52].

4.2.3 Accelerated life aging test

Accelerated life aging tests are highly used when the lifetime of an electrical insulation system is to be decided. As it should last for at least 30 years, observing the different stresses over this timeline is cumbersome. Hence, the stresses are rather increased beyond the operating situation for a shorter period of time. IEC 60505 suggests accelerated tests at a minimum of three different voltage levels [37]. Based on these results, a lifetime curve can be developed.

Not all stresses will be observed under an accelerated life aging test. Some aging factors develop over time and will only be seen after several years [53]. Lifetime curves are hence no guarantee to how the life of an electrical insulation system will unfold, but more of a guidance.

4.3 Experimental setup

The testing was performed at two temperature levels, presented in Table 4.1. At room temperature, partial discharge (PD) tests and breakdown (BD) tests were performed. Next, the temperature was increased to 70 °C, and BD tests together with accelerated aging tests were executed. The temperature was increased due to the desired simulation of the real-life thermal condition the insulation in the modular machine will experience.

Table 4.1: Overview over which test is performed at what temperature.

Test temperature	Partial discharge test	Breakdown test	Accelerated aging test
Room temperature	x	x	
70 °C		x	x

As these type of tests operate in a stochastic manner, three test objects were used for each test. That is, three epoxy cups with silica filler and three epoxy cups without silica filler.

Different experimental setups were used in the two test temperatures. Similar for them was the use of an isolator tank where the test objects were situated in. An earthed electrode was at the bottom inside both of the tanks. The cup was positioned on this electrode, and a high voltage electrode was added at the top such that the cup was situated between them.

One of the common denominators for the different tests was the voltage source. A clean voltage transition when ramping up the voltage was realized for both setups with the help of a MATLAB script and a DAQ card (NI USB-6216), such that each test was identical when it came to the applied voltage.

The approach and experimental setups for the testing will now be presented. The subsections are divided into the two test temperatures, testing at room temperature and testing at 70 °C. The tests performed under each condition are further elaborated, and the order of presentation correlates to the chronological order the tests were performed at.

4.3.1 Testing at room temperature

A flow diagram of the approach at room temperature is seen in Figure 4.6. The main objective of the partial discharge (PD) tests conducted at room temperature was to quality check the cups and sort out the test objects that exhibited undesired characteristics. Regarding the breakdown (BD) tests, a comparison between BD tests at room temperature and at 70°C was made.

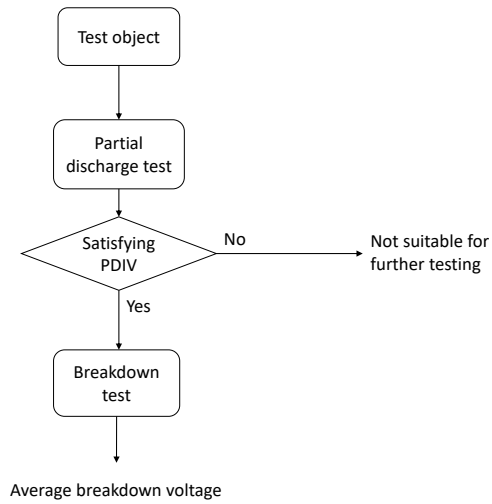


Figure 4.6: Flow diagram of the approach performed at room temperature.

Partial discharge test

A good indicator of whether a test object is suitable for further testing is to observe partial discharge inception voltage (PDIV) in the insulation [54]. If the PDIV of a test object is low, the quality of the test object is likely bad with a poor withstand strength. By observing PRPDA patterns, the PDIV for the test objects can be decided.

The test circuit for the partial discharge tests is presented in Figure 4.7. The conventional partial discharge measurements proposed by IEC 60270 were used. The test cell consisted of the insulator tank with the test object. It was in parallel with a coupling capacitor, C_k and a measuring impedance, CPL 542. The measuring impedance was connected to a MPD 600, which was suited for recording and detecting partial discharges. The measurement was then connected to a laptop, where the partial discharges in a PRPDA plot were observed.

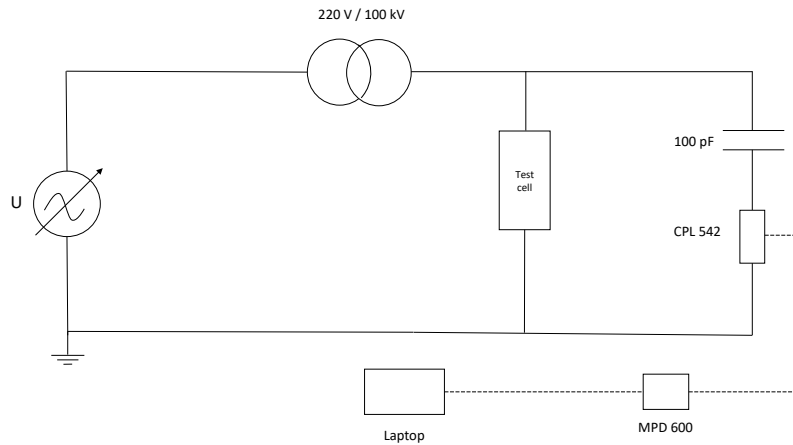


Figure 4.7: The circuit for the partial discharge tests, the physical setup is seen in Figure 4.8 [24].

The coupling capacitor size should be larger than the capacitance of the cup [51]. By assuming the cups have an approximately parallel plane capacitor configuration, the capacitance of each cup was calculated to be 60.8 pF [24]. This was hence an approved size as the coupling capacitor was 100 pF.

Figure 4.8 shows the experimental setup for the PD tests. The tank was filled with MIDELE 7131. This was to avoid creeping currents.

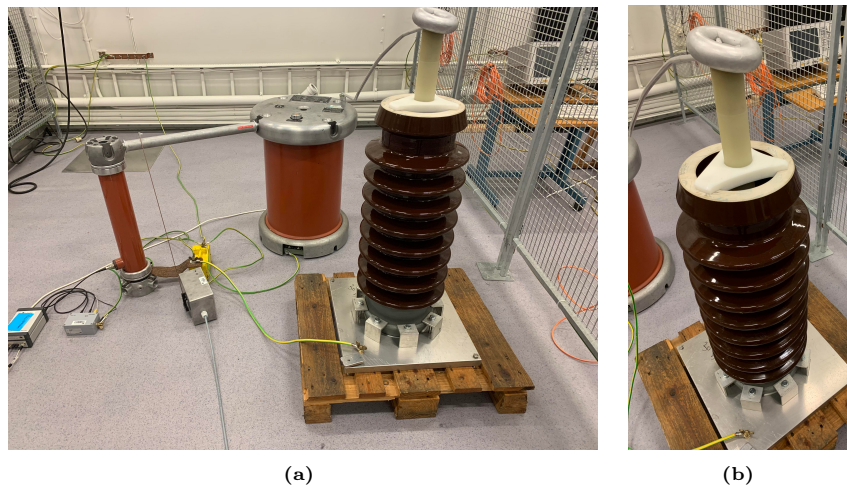


Figure 4.8: The experimental setup used for the testing of the test objects at room temperature: (a) Complete setup for the partial discharges tests; (b) Close-up of the test cell.

Test objects from different castings were tested such that if there were any differences in the different castings, they would be spotted. They are presented in Table 4.2. The cups were numbered based on the cup and casting number. The cup number was given digit numbering, while the casting number was given letter numbering. As an example was cup 2A the second cup made in the first casting. Further were the cups

divided into epoxy cups with and without silica filler. The test objects were examined with a microscope, this is presented in Appendix C.

Partial discharge (PD) tests were done on three epoxy cups with silica filler and three epoxy cups without silica filler. In addition, were cups that contained flaws and errors tested such that a reference point where made, giving the possibility to make a comparison. A healthy cup will further be defined as a cup possessing no visual cavities, while an unhealthy cup is a cup where cavities can be seen.

Table 4.2: *Test objects chosen for the partial discharge testing at room temperature.*

Epoxy cups without silica filler	Epoxy cups with silica filler
2A	2A 3A Fault: 4A
1B	1B
3C Fault: 2C	

High voltage must be avoided such that no breakdown occurs in the test objects in the partial discharge tests. The voltage was ramped from 5 kV to 20 kV, with a step length of 5 kV, each step lasting for 60 seconds.

Breakdown test

The main objective of the breakdown (BD) tests was to find the maximum withstand voltage. Three cups were tested for the two different cup compositions, and the average breakdown voltage was calculated. The same cups used in the partial discharge test were used for the breakdown test, as seen in Table 4.2.

The setup used in the breakdown test is presented in Figure 4.9. It is similar to Figure 4.7. However, the coupling capacitor was removed from the circuit as no partial discharges were being observed, in addition to the measurement instruments.

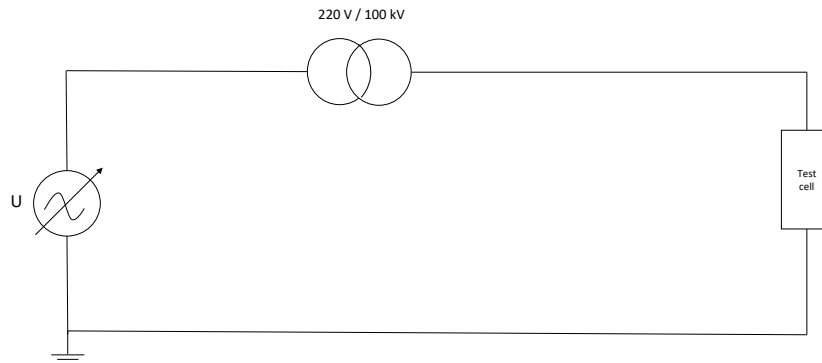


Figure 4.9: *The circuit for the breakdown tests [24].*

The tests were executed by a start voltage of 10 kV with a step length of 2.5 kV. Each voltage steps lasted for 5 minutes. The voltage was increased until a breakdown occurred.

4.3.2 Testing at 70 °C

Figure 4.10 presents the test approach at 70 °C. First, three breakdown tests on the two cup configurations were performed. From that, the average breakdown voltage was calculated. Accelerating aging tests were from this result conducted. The applied voltage was decreased a certain percent from the average breakdown voltage, and the time to breakdown was recorded.

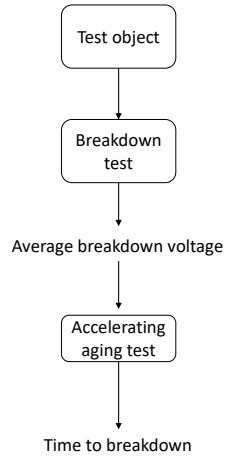


Figure 4.10: Flow diagram of the testing performed at 70 °C.

Breakdown test

The main objective of the BD tests at 70 °C was the same as described in the BD tests at room temperature. However, due to the temperature increase, the average BD voltage also decided the voltage levels used for the accelerated aging tests.

By increasing the temperature to 70 °C, a better simulation of the thermal state in the insulation of the modular machine was created. These BD voltage results will hence be more representative of the machine compared to the BD voltage found at room temperature.

A new experimental setup was used, seen in Figure 4.11. The same circuit presented in Figure 4.9 applied also for the breakdown (BD) tests performed at 70 °C. The only difference was the test cell. The fluid inside the isolator tank at 70 °C was NYTRO 10XN. The difference in the type of fluid compared to the MIDEL used at room temperature was due to practical reasons, as the tanks were already filled with their respective fluids when the takeover of the tanks took place.

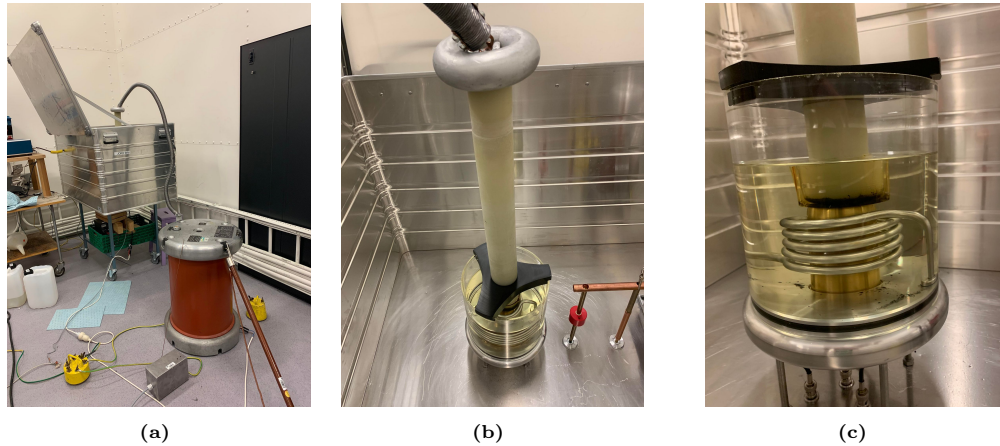


Figure 4.11: The setup used for the testing of the test objects at 70 °C: (a) Complete setup for the breakdown tests and accelerated aging tests; (b) The test cell; (c) Close-up of the test cell with the NYTRO 10XN and a cup situated between the two electrodes. A heating coil made it possible to increase the temperature in the oil above room temperature.

A lower breakdown voltage was assumed to occur at 70 °C compared to at room temperature. However, a start voltage of 10 kV with a step length of 2.5 kV was still used.

The cup used in the breakdown tests is presented in Table 4.3. The same numbering of the cups presented in Table 4.2 applies.

Table 4.3: Test objects chosen for the breakdown testing at 70 °C.

Epoxy cups	Epoxy cups with silica flour
	Cup 5A
Cup 2B	Cup 2B Cup 3B
Cup 4C	
Cup 1D	

Accelerated aging test

For the accelerated aging tests, the same setup as the BD tests was used, seen in Figure 4.11.

The average BD voltage obtained from the BD tests at 70 °C decided the voltage levels at the accelerated aging tests. In the accelerated aging tests, the voltage was decreased to a level just below the average breakdown voltage. The time to breakdown was thereafter observed.

The first voltage level was set to 90 % of the average BD voltage. It was decided to observe the time to breakdown under this voltage level before the next voltage level decrease was chosen.

5 Test results and discussion

The results obtained from the methodology described in Chapter 4 will now be presented, in addition to a discussion regarding them. The sections are divided into partial discharge tests, breakdown tests and accelerated aging tests.

5.1 Partial discharge test

In addition to the assumed healthy test objects, PD tests were also performed on unhealthy cups. This gave the opportunity to make a comparison between healthy and unhealthy cups.

The results regarding the PD tests are further divided into epoxy cups with and without silica filler.

5.1.1 Epoxy cups without silica filler

Table 5.1 presents the average partial discharge inception voltage (PDIV) and the average of the maximum discharge in the three tests performed at each epoxy cup without silica filler.

Table 5.1: Average partial discharge inception voltage (PDIV) and average maximum discharge of three partial discharge tests at each epoxy cup without silica filler observed in the PRPDA plot.

Cup	PDIV [kV]	Maximum discharge [pC]
2A	15	66.0
1B	10	101.9
3C	20	161.1
Faulted cup	10	445.0

The PDIV values range from 10 to 20 kV. The precise PDIV of the cups might be closer to each other due to the high voltage step length of 5 kV.

Cup 3C had the highest PDIV of 20 kV. This was also the healthy cup with the highest discharge magnitude peak. Cup 2A had a PDIV at 15 kV but the lowest discharge magnitude. From the PDIV, it can be argued that cup 3C possessed the greatest withstand strength.

As 1B had the lowest PDIV, it was assumed that this cup might experience an earlier breakdown compared to the other cups. The PDIV of the faulted cup was the same as cup 1B at 10 kV. The faulted cup had an unintentional breakdown at 18.38 kV. However, no BD occurred in cup 1B at this voltage level. Cup 1B possessed a greater withstand strength than the faulted cup.

With an increased voltage, the discharge magnitude increased. To initiate a discharge, a start-electron must be present when the voltage over the cavity rises above the Pachen voltage. When the voltage is increased, the voltage over the cavity also increases accordingly. The discharge will thus be larger as the voltage across the cavity will be higher when the start-electron appears.

When observing the PRPDA plots for the healthy cups, no clear voids were spotted. However, some symmetry was seen in both half periods in addition to the discharge starting at zero crossing and ending at peak. It can hence be debated whether the cups possessed voids. Even though no clear PD pattern for voids was observed in the PRPDA plot, it does not necessarily mean no voids were present in the test objects. However, the discharges seen could also have occurred in the oil as gas bubbles might have accumulated. A better interpretation of the PDs could have been made if each voltage step lasted longer than 60 seconds, as the potential gas bubbles would have dissipated over time. If PDs in the test objects were present, the discharges would continue to arise in the PRPDA plot regardless of the voltage step time.

Figure 5.1 presents the PRPDA plot of epoxy cup 2A. In the faulted cup, a better symmetry in the PRPD patterns was observed, hence PDs in the void were likely to have occurred.

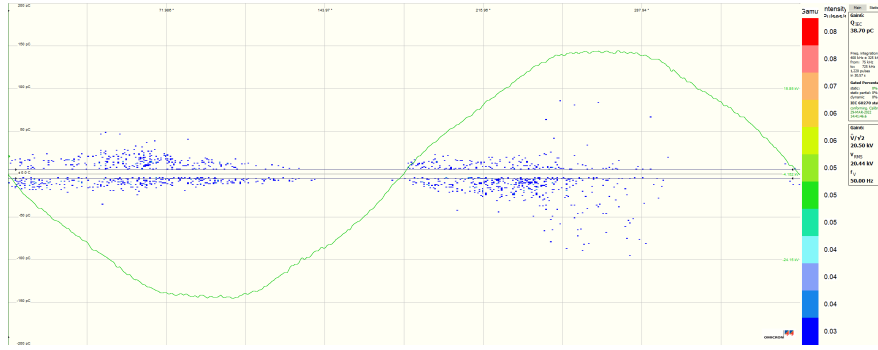


Figure 5.1: PRPDA plot of epoxy cup 2A showing no clear PD pattern for voids.

5.1.2 Epoxy cups with silica filler

Table 5.2 present the average partial discharge inception voltage (PDIV) and average maximum discharge of three partial discharge tests at each epoxy cup with silica filler.

Table 5.2: Average partial discharge inception voltage (PDIV) and average maximum discharge of three partial discharge tests at each epoxy cup with silica filler.

Cup	PDIV [kV]	Maximum discharge [pC]
2A	15	470.1
3A	10	822.6
1B	5	1230.0
Faulted cup	5	173.8

Cup 1B had the lowest PDIV together with the faulted cup. The faulted cup had a surprisingly low maximum discharge magnitude compared to the healthy cups. It must be addressed that the maximum applied voltage at the cup was 15 kV to avoid unwanted breakdown. However, the discharge magnitude was still low. Observing the PRPDA patterns in the faulted cup, characteristics of voids were seen, correlating well with what was observed under the examination of the cup, seen in Appendix C. Regarding cup 1B, no clear symmetry was spotted in the PRPDA plot. Hence no conclusion on whether the cup had cavities can be made.

The maximum discharge magnitude in the healthy epoxy cups with silica filler was far more significant than the epoxy cup without silica filler, but between them, variation also occurred. Cup 2A had the lowest magnitude at 470.1 pC, and cup 1B had the highest at 1.23 nC. In this case, the cup with the highest PDIV had the lowest maximum discharge magnitude. Cup 2A would likely have the highest BD voltage, and cup 1B the lowest due to the PDIV values.

The PRPDA patterns in cups 2A and 3A clearly showed PDs occurring in voids. The PRPDA patterns in cup 2A can be seen in Figure 5.2. As mentioned regarding cup 1B, no symmetry was spotted. As cup 2A and 3A were produced in the same casting, the procedure in this particular casting might have led to the cavities that easily arise in the PRPDA plot. The pressure chamber in casting procedure A for the epoxy cups with silica filler were not turned on during curing. This is described in Appendix B. This could have played an essential part in formation of voids in these cups.

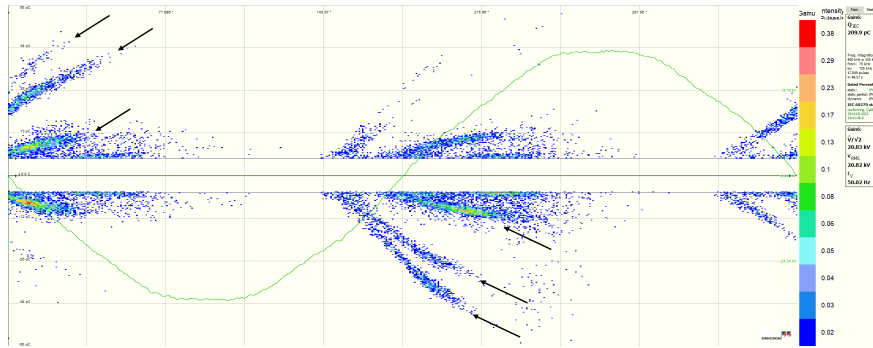


Figure 5.2: PRPDA pattern of cup 2A. At least three voids with different sizes can be observed, marked with black arrows.

5.1.3 Summary of discussion regarding PD results

Discharge patterns differ in the PRPDA plots in the epoxy cups with and without silica filler. No clear symmetry can be spotted in the epoxy cups without silica filler. Despite this, no conclusion regarding whether PDs in voids occurred is possible to make. However, regarding the epoxy with silica cups, a clearer symmetry indicates voids in the test objects.

A notable difference in PDIV occurred in the epoxy cups with and without silica filler. The epoxy cups with silica filler experienced a lower average PDIV compared to the epoxy cups without silica filler. It is reasonable to conclude that adding silica filler reduced the PDIV of the test objects, as no other changes were made. There are two possible reasons for this deviation. The first possibility is poor blending in the mixture when adding the silica flour. Even though the mixing was performed with ultrasound, it might not have been sufficient such that cavities might have been formed in the test objects. The second reason could have been due to the silica flour size, as the one utilized had micro-sized particles. As mentioned in Section 2.1.3, research has stated that micro-sized silica flour decreases the withstand strength. From the PDIV results, it can be expected that the epoxy cups with silica filler will have a poorer withstand strength in the BD tests compared to the epoxy cups without silica filler.

A source of error regarding the PD tests is the voltage step length. This should have been smaller such that more precise PDIV values were obtained. The voltage step time should have been longer, so potential gas bubbles in the oil had time to cease. This would have made it possible to determine if the epoxy cups without silica filler possessed cavities.

5.2 Breakdown test

Table 5.3 presents the results obtained from the breakdown tests in the epoxy cups with and without silica filler. The average breakdown voltage was calculated from the breakdown voltage at each cup and is shown in the table.

Table 5.3: Breakdown voltage and average breakdown voltage of epoxy cups with and without silica filler at room temperature and 70 °C.

	Breakdown voltage [kV]						Average breakdown voltage [kV]	
	Room temperature			70 °C			Room temperature	70 °C
Cup	2A	1B	3C	4B	4C	1D		
Epoxy cup without silica filler	46.5	34.1	44.2	33.9	33.8	36.4	41.6	34.7
Cup	2A	3A	1B	5A	2B	3B		
Epoxy cup with silica filler	37.0	26.8	31.9	35.8	31.0	38.7	31.9	35.2

In the epoxy cups without silica filler, a decrease of 16.6 % in average breakdown voltage occurred when increasing the temperature to 70 °C. This coincides well with Section 2, where research stated that a decrease in withstand strength occurs with increased temperature.

Regarding the epoxy cups with silica filler, there was no decrease in average BD voltage when the temperature increased. The average BD voltage increased when the temperature increased. Due to the addition of silica filler, the epoxy cups with silica filler withstood an increasing temperature better compared to the epoxy cups without silica filler.

When comparing the two cup configurations against each other at the same test temperature, the epoxy cups without silica filler have the greatest withstand strength at room temperature with 23 % higher average breakdown voltage compared to the epoxy cups with silica filler. This is not surprising as the silica flour used for the epoxy with silica cups has micro-sized particles. The results also match well with the results obtained in the PD testing. In addition to the size of the silica flour, other factors might have affected the BD voltage in the epoxy cups with silica filler. The silica flour might not have been blended enough such that cavities have been formed. In addition, could the volume percent played a part. The mixture consisted of 65 wt. % silica flour. However, the parts per weight of each material match the data sheet (Appendix B) and should hence be an acceptable ratio. Another factor could be related to the environmental condition when testing. However, it is unlikely as the tests were conducted on the same day.

At 70 °C, no significant deviation was observed in the average BD voltage between the epoxy cups with and without silica filler. However, a more considerable variation in BD voltage at each cup in the epoxy cups with silica filler occurred compared to those without silica filler. Casting process B for the epoxy cups with silica filler had both the lowest and highest BD voltage at 70 °C. It seems that what cup that experience a poor withstand strength was arbitrary, correlating well with the stochastic behavior these tests are associated with.

In the epoxy cups without silica filler at room temperature, the most deviating BD voltage compared to the other cups was the BD voltage at cup 1B. This cup's withstand strength was far poorer than cups 2A and 3C. This matches the anticipation after the PD testing that the low PDIV correlated to a low withstand strength. After the early breakdown in cup 1B, an examination of the cup was done. Figure 5.3 shows a cut of the cup and where the breakdown channel went.

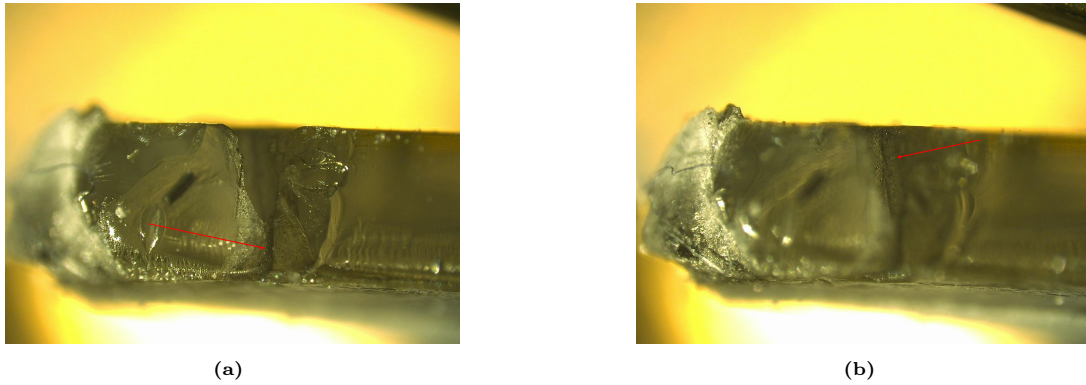


Figure 5.3: Examination of epoxy cup 1B without silica filler. Note the red arrow pointing at the breakdown channel.

As the area had melted due to the breakdown, it was difficult to determine the cause. It can hence not be drawn any conclusion regarding why this cup failed at a sooner voltage level compared to the other tests other than that cup 1B showed a lower PDIV. The average BD voltage was decreased due to the BD voltage in cup 1B. However its BD voltage was far higher than the BD voltage at the faulted epoxy cup without silica which was 18.38 kV. This confirms that cup 1B had a greater withstand strength than the faulted cup.

Epoxy cup 3A with silica filler at room temperature had the lowest BD voltage at 26.8 kV. This might be due to the voids observed in the PRPD pattern. However, voids were also observed in the PRPD pattern in cup 2A, but its BD voltage was the highest among the cups. Another interesting observation regarding epoxy cup 3A and 2A with silica filler was that even though they were produced in the same casting process, in addition to the pressure chamber not being turned on during curing, their difference in BD voltage was significant.

To validate the results after breakdown, the cups were examined. All the cups tested at the BD tests had been ruptured at the bottom of the cup. However, there was a tendency that the majority had experienced breakdowns close to the corners of the cup. This is likely due to the higher electric field stresses in these areas.

It could be argued that the PD testing should have been done at the cups at 70 °C as well. Even though the results in the BD tests at room temperature had a significant deviation, the PD tests gave a better understanding to why the cups behaved as they did in the BD tests. When only performing BD tests without first checking them for PDs, this vital information was lost at 70 °C.

The stochastic relation makes it challenging to find a suitable average BD voltage for the cups. If more test objects were made and tested, a better average BD voltage would have been obtained. This would have given a better starting point for the voltage level decisions in the accelerated aging tests. However, as the production of the test objects was time demanding, it was not possible due to the time limitation.

5.3 Accelerated aging test

The accelerated aging tests were first performed on the epoxy cups without silica filler. The voltage level was set to 90 % of the average BD voltage in the epoxy cups without silica filler at 70 °C, seen in Table 5.3. This coincided with an applied voltage of 31.2 kV.

Cup 3B was the first cup to be tested. The breakdown occurred after 13.33 hours. However, after examining the cup, it was observed that the BD channel was situated at the cup wall. The BDs had to occur at the bottom of the cup to get a valid result in the accelerated aging tests. This was due to the homogeneous electric field distribution that was located there. Hence, the result could not be used in the further estimation of the lifetime of the insulation material.

Afterward, cup 2D was tested. It took 9.88 hours until a BD occurred. However, the same undesirable breakdown location as cup 3B took place in this cup. Hence, the result was not valid for the further establishment of lifetime curves. The examination of cup 2D is seen in Figure 5.4. The same was found in the examination of cup 3B.

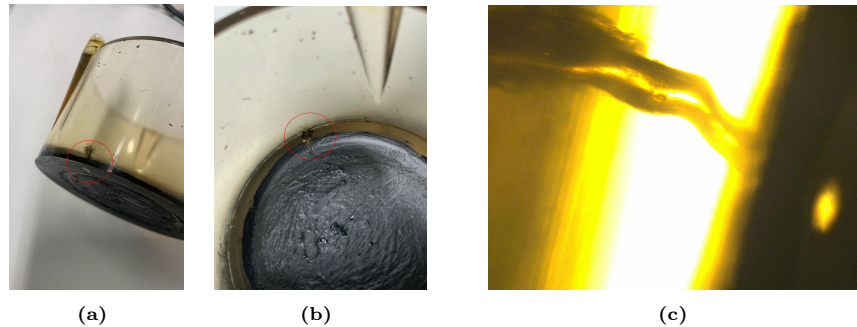


Figure 5.4: Examination of epoxy cup 2D after breakdown after 9.88 hours. The breakdown is marked in red in (a) and (b).

After the two unsuccessful attempts, it was decided to coat the cup walls better. The varnish was painted a bit higher up on the wall than before. The wanted outcome of this was to decrease the electric field stresses around the corners of the cup such that no breakdown took place in the inhomogeneous field areas.

Cup 3D was then tested. Several voltage interruptions took place under this testing. The first interruption occurred after 28.42 hours. After the interruption, the voltage was again applied over the cup. A MATLAB script was used to ramp up the voltage and keep it fixed at the desired voltage level. The time set for how long the applied voltage of 31.2 kV should stay put was 48 hours. However it turned out that this was a too short time period as no BD occurred. Hence, the time period was increased to one week. After one week, a breakdown had still not occurred in cup 3D. After this, it was determined to do no further experiments on this cup. This was due to the considerable electric stress the cup had been exposed to, and the time to breakdown would not have been a valid result.

The voltage level was decided to be increased to 95 % of the average BD voltage to obtain a valid time to breakdown value. This coincided with an applied voltage of 32.9 kV. Cup 4D was first tested and experienced a breakdown after only 3.6 minutes. The BD occurred at the bottom of the cup, it was hence a valid result. However, it can be discussed whether the cup possessed an undiscovered cavity.

Cup 6D was then tested. After one week, no breakdown occurred in the cup. Due to this result, cup 4D likely had a premature failure as presented in the bath tube curve in Figure 2.2. It could hence not be further used in the development of lifetime curves.

Even though the breakdown in the BD tests occurred at the bottom of the cups, the breakdown in the accelerated aging tests for the first two cups occurred in the walls. The inhomogeneous electric field was

a contributing factor to BD when the maximum withstand voltage was not applied. When painting the semiconducting varnish a bit higher on the walls of the cups, no BD occurred at the walls in the time perspective available to do the experiments.

Another way to decrease the time to breakdown is by increasing the frequency. However, this was not considered in this work. IEC 60505 states that a frequency increase over operation state can be used when conducting accelerated aging tests when having electrical stress as the single aging factor [37].

Aging tests are time demanding. As the two first epoxy cups were invalid in addition to voltage interruptions, important time was lost. By painting the semiconducting varnish high up at the cup walls, the time to breakdown increased. Due to the short time perspective, no accelerated aging tests on epoxy with silica flour cups were performed, nor was the establishment of lifetime curves possible to obtain.

5.4 Sources of error

For each test, 3 cups were utilized. As seen from the results, the deviation in some cases is significant. Hence more cups should have been used to get a more precise result when calculating the average value. The casting is a slow process that requires a lot of time, which is why no more cups were produced.

As an experienced producer did not make the cups, the cups might contain impurities and voids not desirable for an insulation material. However, fabric-made insulation materials are rarely perfect. It could be argued that due to their flaws, they represent the real-life situation when working with electrical insulation.

A possible source of error regarding the experimental setup is that contamination from the semiconducting varnish was attached to the electrodes after a breakdown. If this pollution was not washed well enough off after each breakdown, it could have played a part in the PD and BD voltage in a negative way.

As the test temperature at 70 °C coincides best with the actual operating state of the modular HVDC machine, how the cups performed at this temperature weights more compared to the tests performed at room temperature. However, no significant deviation in the average BD voltage between the epoxy and epoxy with silica flour cups is found at 70 °C. Hence it is difficult to conclude the best performing cup configuration. It must, however, be addressed that the epoxy cups with silica filler withstood the temperature increase better compared to the epoxy cups without silica filler. Hence it could be assumed that a further increase in temperature will give an even poorer average BD voltage in the epoxy cups without silica, and that adding silica flour will resist the temperature change better.

When performing accelerated aging tests, other unwanted phenomena than aging processes can be triggered. This could have affected the test objects and given unrealistic results. On the other hand, it is also likely that typical, wanted aging processes were avoided when performing these tests due to the short time span. Hence the results obtained in the accelerated aging tests are uncertain and should only be used as guidance when deciding the lifetime of an electrical insulation system.

As electric stress is assumed to be the only aging factor, the cups might exhibit excellent properties when dealing with the other TEAM stresses. How the addition of silica filler has affected these properties has not been examined.

6 Conclusion

This thesis aimed to establish lifetime curves for a DC insulation system for a modular HVDC generator. However, due to the time limitation, it was not accomplished. Poor painting of the semiconducting layer and several voltage interruptions gave invalid results. When the corners of the cups were coated better, the time to breakdown increased both at 95 % and 90 % of the average BD voltage at 70 °C, giving no results that could be used in the further development of lifetime curves.

Despite this, other results from PD and BD tests were obtained at AC. In addition, was a methodology made. They can be used in further developing the DC insulation system for the modular HVDC machine.

PD testing was a good way to predict the withstand strength of the test objects by monitoring the PDIV. However, it was challenging to decide the precise PDIV, due to the large voltage step length and the uncertainty when spotting discharges in a PRPDA plot.

At room temperature, the average BD voltage of the epoxy cups without silica filler was 23 % higher compared to the epoxy cups with silica filler. This was likely due to the micro-sized particles in the silica flour. However, a poor blending of the silica flour could also have affected the results. At 70 °C, no remarkable difference between the two cup configurations was found. This was due to the epoxy cups with silica filler, as their average BD voltage did not decrease as expected. The epoxy cups without silica filler, on the other hand, had a decrease of 16.6 % when increasing the temperature to 70 °C.

7 Experience and further work

The development of lifetime curves of an insulation system is a time-consuming task. The time span of a master thesis makes it a challenging mission. Several important topics for a further establishment of an insulation system for a modular HVDC generator were not researched in this thesis. These will be presented. In addition, will some experience and typical pitfalls be addressed.

- If lifetime curves are to be made in a master thesis, the making of the test object must begin during the specialization project a year before submitting the final thesis. As the casting of the test object occupies essential time, it should be done earlier such that as much time as possible is given to the accelerated aging tests.
- The further development of lifetime curves for the insulation material at AC should be done. After this is accomplished, the same testing and development should be done at DC. When this is fulfilled, the design of the insulation system specifically for the modular HVDC machine can be made and tested.
- Regarding the insulation material used in this thesis, they were chosen, among other things, due to their easy availability when deciding the test object configuration. Other materials that could be suitable for the insulation system should hence be explored.
- A further investigation regarding why the average BD voltage of the epoxy cups with silica filler did not decrease when increasing the temperature should be done. Whether the silica flour gave the insulation system a better withstand strength when increasing the temperature would be interesting to explore.
- As only micro-sized silica particles were used as filler, it would be interesting to observe the effect of nano-sized silica particles as filler.
- Only electric stress was used as the single aging factor in the tests. Other stresses must also be investigated before a complete insulation system can be made for the modular HVDC generator. Especially is the mechanical impact an important part when designing an insulation system. Multi-factor aging tests could also be performed.
- Whether a more optimal silica flour ratio can be found could be researched.

References

- [1] Sofie Barmen Stein. “Design Procedure for a Modular HVDC Generator for Offshore Wind”. Specialization project. Unpublished. 2021.
- [2] United Nations. *Adoption of the Paris Agreement*. 2015.
- [3] Farhan Hai Khan et al. “Wind Energy: A Practical Power Analysis Approach”. In: *2021 Innovations in Energy Management and Renewable Resources(52042)*. 2021, pp. 1–6.
- [4] Rennian Li and Xin Wang. “Status and challenges for offshore wind energy”. In: *2011 International Conference on Materials for Renewable Energy Environment*. Vol. 1. 2011, pp. 601–605.
- [5] T.K. Vrana et al. “Impact of present and future HVDC links on the Nordic power grid”. In: *13th IET International Conference on AC and DC Power Transmission (ACDC 2017)*. 2017, pp. 1–6.
- [6] Pål Keim Olsen et al. “A Transformerless generator-converter concept making feasible a 100 kV light weight offshore wind turbine: Part I - The generator”. In: *2012 IEEE Energy Conversion Congress and Exposition (ECCE)*. 2012, pp. 247–252.
- [7] Regjeringen. *Opner området for havvind i Noreg*. 2020.
- [8] Regjeringen. *65 millioner kroner til havvind-undersøkingar*. 2022.
- [9] Pål Keim Olsen. *Full proposal ModHVDC*. Aug. 2018.
- [10] Runar Mellerud. *Analysis of Losses and Radial Vibration in a PM Synchronous Machine with Physical Modularity*. June 2021.
- [11] Sverre S. Gjerde, Paal Keim Olsen, and Tore M. Undeland. “A transformerless generator-converter concept making feasible a 100 kV low weight offshore wind turbine Part II - The converter”. In: *2012 IEEE Energy Conversion Congress and Exposition (ECCE)*. 2012, pp. 253–260.
- [12] Nancy Frost, Michael Chapman, and Rudolf Bruetsch. “Considerations for Rotating Low-Voltage Machine Insulation Designs”. In: *Conference Record of the 2008 IEEE International Symposium on Electrical Insulation*. 2008, pp. 571–574.
- [13] Marta Husebø. *Study of Mechanical Load Cases and Future Digital Twin Implementation of the Mod-HVDC Generator*. Dec. 2018.
- [14] Greg C Stone et al. *Rotating Machine Insulation Systems*. John Wiley and Sons, Ltd, 2014. Chap. 1, pp. 1–46.
- [15] Hossein Ghorbani et al. “Long-term conductivity decrease of polyethylene and polypropylene insulation materials”. In: *IEEE Transactions on Dielectrics and Electrical Insulation* 24 (June 2017), pp. 1485–1493.
- [16] F.H Kreuger. *Industrial High DC Voltage*. Delft University Press, 1995.
- [17] Saliha Abdul Madhar et al. “Study of DC partial discharge on dielectric surfaces: Mechanism, patterns and similarities to AC”. In: *International Journal of Electrical Power and Energy Systems* 126 (Mar. 2021), p. 106600.
- [18] Thomas Christen. “Characterization and robustness of HVDC insulation”. In: June 2013, pp. 238–241.
- [19] S. Delpino et al. “Feature article - Polymeric HVDC cable design and space charge accumulation. Part 2: insulation interfaces”. In: *IEEE Electrical Insulation Magazine* 24.1 (2008), pp. 14–24.
- [20] Greg C. Stone et al. *Electrical Insulation for Rotating Machines*. John Wiley and Sons, Ltd, 2014. Chap. 1, pp. 1–46.
- [21] Pål Keim Olsen. *Insulation System of Rotating Machine - Analysis of an Offshore Wind Turbine Generator*. June 2008.
- [22] Juha Pyrhonen, Tapani Jokinen, and Valeria Hrabovcova. *Design of Rotating Electrical Machines*. John Wiley and Sons, 2009. Chap. 8.
- [23] Thomas Christen, Lise Donzel, and Felix Greuter. “Nonlinear Resistive Electric Field Grading Part 1: Theory and Simulation”. In: *Electrical Insulation Magazine, IEEE* 26 (Jan. 2011), pp. 47–59.
- [24] Erling Ildstad. *TET4160 Insulating Materials for High Voltage Applications*. First edition. NTNU - Department of Electric Power Engineering, 2020.

- [25] Wang Qi et al. “The thermal conductivity and electrical strength of epoxy resin with different filler content of micro and nano alumina”. In: *2012 IEEE International Conference on Condition Monitoring and Diagnosis*. 2012, pp. 1110–1113.
- [26] Abdullahi Mas’ud et al. “Electrical Properties of Different Polymeric Materials and their Applications: The Influence of Electric Field”. In: May 2017.
- [27] Rachid Hsissou. “Review on epoxy polymers and its composites as a potential anticorrosive coatings for carbon steel in 3.5% NaCl solution: Computational approaches”. In: *Journal of Molecular Liquids* 336 (2021), p. 116307.
- [28] Thomas W. Dakin. “Application of Epoxy Resins in Electrical Apparatus”. In: *IEEE Transactions on Electrical Insulation* EI-9.4 (1974), pp. 121–128.
- [29] Santanu Singha and M. Joy Thomas. “Dielectric properties of epoxy nanocomposites”. In: *IEEE Transactions on Dielectrics and Electrical Insulation* 15.1 (2008), pp. 12–23.
- [30] Ramesh Talreja and Janis Varna. *Modeling Damage, Fatigue and Failure of Composite Materials*. Woodhead Publishing Series in Composites Science & Engineering, 2016. Chap. 1.
- [31] Mitja Linec and Branka mušič. “The Effects of Silica-Based Fillers on the Properties of Epoxy Molding Compounds”. In: *Materials* 12 (June 2019), p. 1811.
- [32] P.L. Teh et al. “The properties of epoxy resin coated silica fillers composites”. In: *Materials Letters* 61.11 (2007), pp. 2156–2158.
- [33] Takahiro Imai et al. “Effects of Epoxy/Filler Interface on Properties of Nano or Micro-composites”. In: *Ieej Transactions on Fundamentals and Materials* 126 (May 2006), pp. 84–91.
- [34] Toshikatsu Tanaka. “Dielectric Nanocomposites with Insulating Properties”. In: *Dielectrics and Electrical Insulation, IEEE Transactions on* (Nov. 2005), pp. 914–928.
- [35] Yujie Hu et al. “Some mechanistic understanding of the impulse strength of nanocomposites”. In: *2006 IEEE Conference on Electrical Insulation and Dielectric Phenomena*. 2006, pp. 31–34.
- [36] Michele Preghenella, Alessandro Pegoretti, and Claudio Migliaresi. “Thermo-mechanical characterization of fumed silica-epoxy nanocomposites”. In: *Polymer* 46.26 (2005), pp. 12065–12072.
- [37] IEC 60505. *Evaluation and qualification of electrical insulation systems*. July 2011.
- [38] Philip Kosky et al. “Chapter 11 - Industrial Engineering”. In: *Exploring Engineering (Fifth Edition)*. Ed. by Philip Kosky et al. Fifth Edition. Academic Press, 2021, pp. 229–257.
- [39] Gian Montanari et al. “Ageing and Reliability of Electrical Insulation: The Risk of Hybrid AC/DC Grids”. In: *High Voltage* 5 (Oct. 2020).
- [40] Bishal Silwal and Peter Sergeant. “Thermally Induced Mechanical Stress in the Stator Windings of Electrical Machines”. In: *Energies* 11.8 (2018).
- [41] Yongzhe Tang et al. “Temperature Effects on the Dielectric Properties and Breakdown Performance of h-BN/Epoxy Composites”. In: *Materials* 12 (Dec. 2019), p. 4112.
- [42] Christof Sumereder, Hans Michael Muhr, and Rudolf Woschitz. “Life time investigations at electric insulation systems, theory and measurements”. In: *DISEE*. Vol. 15. 2004, pp. 28–31.
- [43] Svein Hellesø et al. “Water tree initiation and growth in XLPE cables under static and dynamic mechanical stress”. In: *2012 IEEE International Symposium on Electrical Insulation*. 2012, pp. 623–627.
- [44] IEC 60270. *High-voltage test techniques - Partial discharge measurements*. July 2018.
- [45] L.A. Dissado and J.C Forthergill. *Electrical Degradation and Breakdown in Polymers*. 2008 The Institution of Engineering and Technology, London, United Kingdom, 2008. Chap. 15.
- [46] Eyad A. Feilat. “Lifetime Assessment of Electrical Insulation”. In: *Electric Field*. Ed. by Mohsen Sheikholeslami Kandelousi. Rijeka: IntechOpen, 2018. Chap. 11.
- [47] Eyad Feilat et al. “Breakdown and aging behavior of composite insulation system under DC and AC high voltages”. In: *WSEAS Transactions on Circuits and Systems* 4 (July 2005), pp. 780–787.
- [48] Dimitri Kececioglu and Julie A. Jacks. “The Arrhenius, Eyring, inverse power law and combination models in accelerated life testing”. In: *Reliability Engineering* 8.1 (1984), pp. 1–9.
- [49] Tong Liu et al. “A new method of estimating the inverse power law ageing parameter of XLPE based on step-stress tests”. In: Oct. 2013, pp. 69–72.
- [50] Udo Fromm. *Partial discharge and Breakdown Testing at High DC Voltage*. 1995.

- [51] Lars Lundgaard. *Measurement of Partial Discharges, NTNU-kurs*. Sept. 2008.
- [52] IEC 602431. *Electric strength of insulating materials*. Mar. 2013.
- [53] L.A. Dissado and J.C Forthergill. *Electrical Degradation and Breakdown in Polymers*. 2008 The Institution of Engineering and Technology, London, United Kingdom, 2008. Chap. 3.
- [54] Thibaut Billard, Cédric Abadie, and Bouazza Taghia. “Advanced partial discharge testing of 540V aeronautic motor fed by SiC inverter under altitude conditions”. In: *SAE 2017 AeroTech Congress & Exhibition*. Fort Worth, United States, 2017, pp. 1–17.

A Epoxy casting in cup configuration - approach

A precis casting procedure must be followed to obtain epoxy cups with approximately similar characteristics. In this appendix, the epoxy casting approach is explained such that similar castings can be executed in the future.

The data sheet developed by Vantico Ltd. named "Araldite Casting Resin System" is used for the casting for both the approach presented in this appendix and appendix B.

The casting mold used for making the epoxy cups and the elements it consists of is shown in Figure A.1.

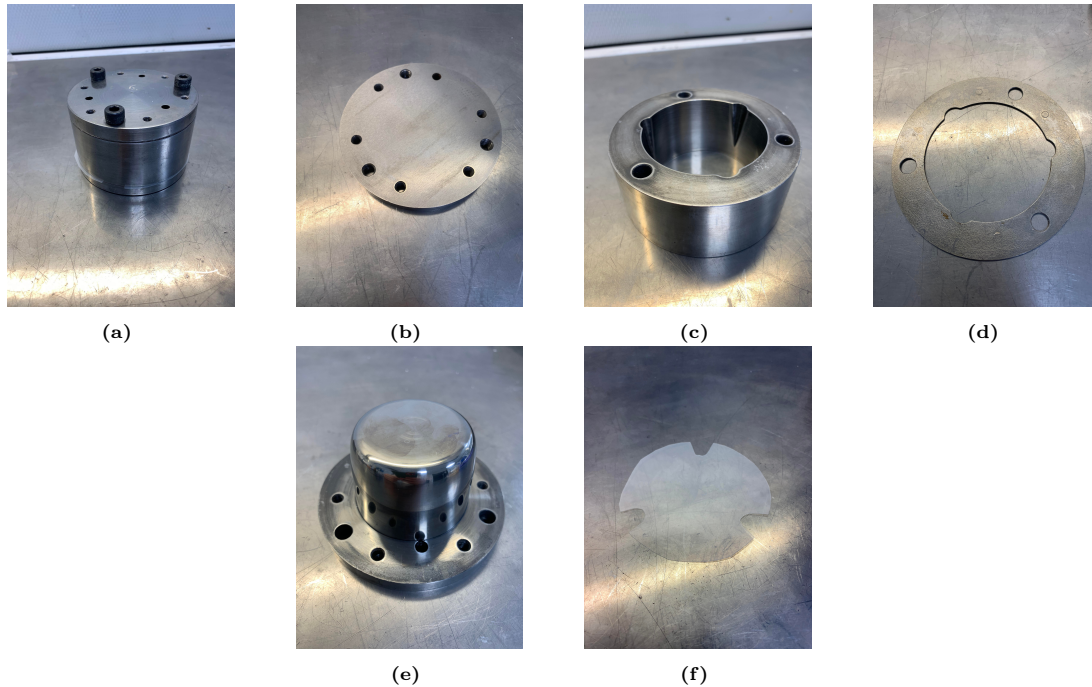


Figure A.1: The casting mold and its components: (a) A complete casting mold together with PET foil; (b) Casting mold element 1; (c) Casting mold element 2; (d) Casting mold element 3; (e) Casting mold element 4; (f) PET foil;

A flow diagram of the casting process is presented in Figure A.2. Each step will be described such that it will be easy to follow the same procedure.

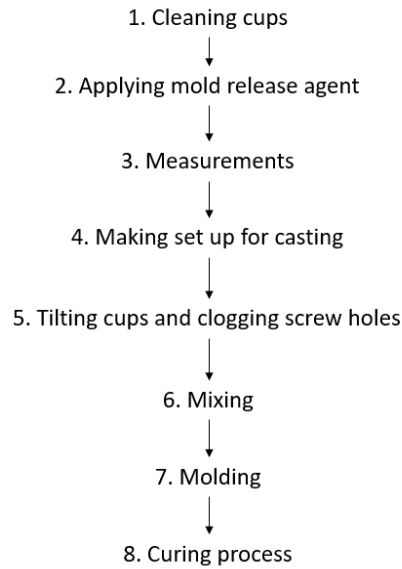


Figure A.2: *Flowdiagram of casting.*

The casting procedure is done with four cup configurations, giving four epoxy cups.

1. Cleaning cups.

The cup configurations used for casting need to be washed. The test objects are cleaned with isopropanol alcohol together with polyester/cellulose wipers. The most important areas to clean are where the mold cup will be in contact with the mixture.

2. Applying mold release agent

To ease the process of separating the components in the test objects from each other after molding, a release agent (Frekote 55-NC) is applied to the surfaces. Another measure to minimize the possibility of the elements being stuck after the curing is by adding circles of PET foil between casting mold element 1 and casting mold element 2 from Figure A.1 (b) and (c) seen in Figure A.3. A release agent must also be added to the PET foil.

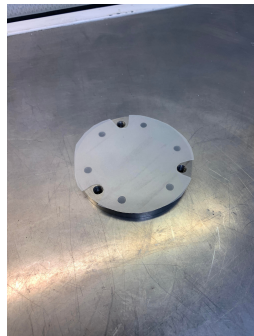


Figure A.3: *PET foil places between casting mold element 1 and 2.*

3. Measurements

The epoxy cups consist of several materials: epoxy, hardener, flexibilizer and accelerator. Each participant is measured parts by weight (pbw), and they are presented in Table A.1. When casting four cups, the recipe is doubled.

Table A.1: Product data and the mixture relation for one epoxy cup portion obtained from the datasheet developed by Vantico Ltd..

Material	Product name	Quantity [pbw]
Liquid, low viscous bisphenol A epoxy resin	Araldite CY228-1	100
Liquid anhydride hardener	Aradur HY 918-1	85
Solvent-free, low viscous polyglycol	Flexibilizer DY 045	17
Liquid tertiary amine accelerator	Accelerator DY 067	0.6

4. Making set up for casting

Then the setup needed for the molding in the vacuum caster chamber is made. It consists of several components such as different tubes, fittings, valves and syringes. The vacuum casting chamber and components with explanations are presented in Figure A.4.

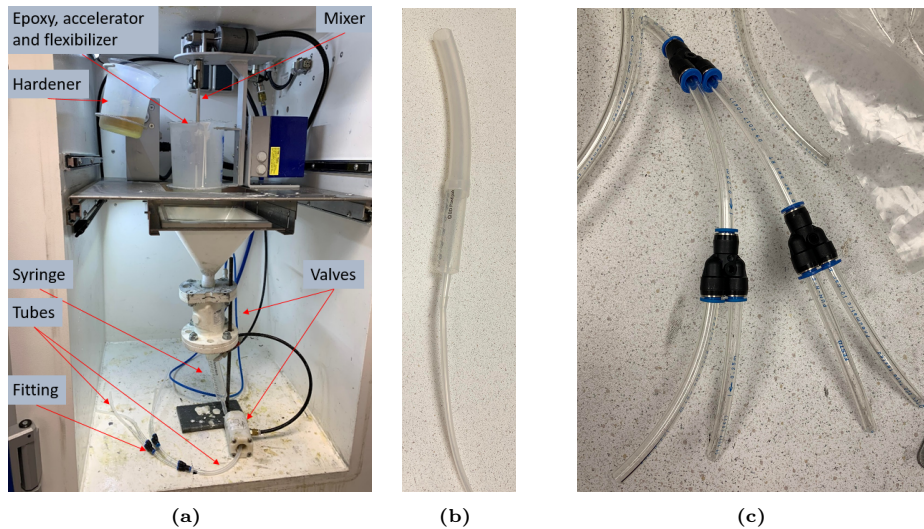


Figure A.4: Components in the vacuum casting chamber: (a) Vacuum casting chamber with explanations ; (b) Tube of silicon connected to a syringe which is attached to the funnel, in addition to a tube of silicon (6 mm) connected to the other end of the syringe; (c) Tubes of glass (6 mm) and fittings make it possible to separate the fluid flow into four cups.

5. Tilting cups and clogging screw holes

The cups are tilted with screws, giving them a more controlled fluid flow. Screw holes are clogged, so no fluid arises at the cup surface. Figure A.5 shows how the cups are made ready for molding.

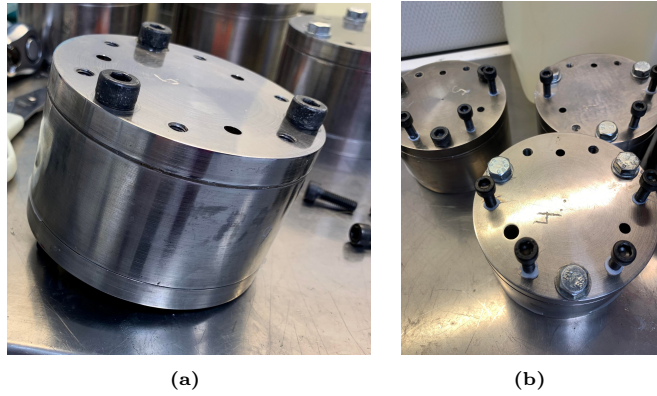


Figure A.5: Making the cups ready for molding: (a) Tilted cup ; (b) Cups clogged with screws.

6. Mixing

The mixture of epoxy, accelerator and flexibilizer is blended for a short period. Afterward, the hardener is combined with the mixture. This blending is more crucial and should at least be done in one and a half hours. It must also be addressed that the mixing is done with a vacuum to prevent air bubbles. Figure A.6 shows the mixer in the solution.



Figure A.6: Mixing.

7. Molding

To fill the cups with the epoxy mixture, the fluid must be pressed through the tubes. This is done by making an air pocket in the syringe seen in Figure A.7.

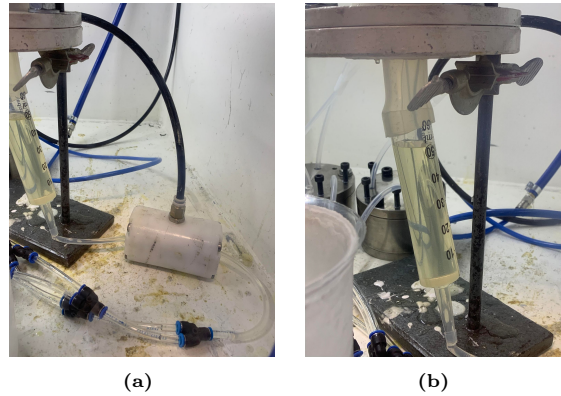


Figure A.7: *Molding and forming of an air pocket in the syringe: (a) Air pocket made in the syringe; (b) Air pocket made in the syringe, zoomed in.*

How an air pocket is made will now be explained. The forming of an air pocket is achieved with the help of the control board seen in Figure A.8.



Figure A.8: *Control board.*

The epoxy mixture is filled in the syringe by tilting down the cup with the mixture. When the syringe is full, the cup is tilted up. Under this proceeding, the casting chamber is in a vacuum, and the tank outlet is closed. In addition, is the tank vacuum on and the tank pressure off. With a filled syringe, the ventilation is set to slow, and the pressure is pressed up to approximately 700 mbar. Then, the tank vacuum is set to off while the tank pressure is turned on. The pressure is then set to about 400 mbar. An air pocket over the mixture in the syringe will arise when the tank outlet is opened, pushing the fluid into the cups. It is important to note that the syringe should not be empty as more air bubbles might arise. Therefore, the tank outlet should be closed before it is empty and a new filling can start. If there are air bubbles in the syringe after the filling, an idea can be to let it be there in a vacuum for some time to mitigate them.

From experience, three filled syringes will be enough to fill the four cups. It is essential to be aware of the tubes placed in the filling holes so that fluid will not spill into the chamber when fluid flows. Figure A.9 shows the molding procedure.

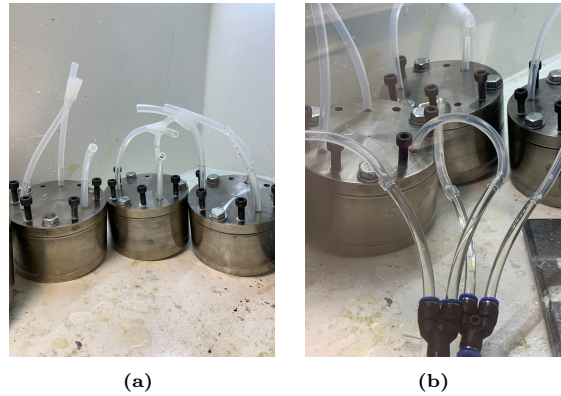


Figure A.9: Molding: (a) Filled cups with fluid arising in the molding holes seen in the tubes; (b) Filling.

8. Curing process

After molding, the curing process starts. This process consists of two steps; pressure chamber and heating chamber. Figure A.10 presents the different chambers used for the curing.

First, the cups are set in a pressure chamber for 4 hours at 15 bar and 80 °C. The goal of the pressure chamber is that by increasing the pressure, air bubbles might cease. A timer should be used and be set to 6 hours due to the inertia in the heating system.

Second, the cups are taken out of the pressure chamber, and the epoxy is released from the casting mold. Then the cups are set in a heating chamber at 140 °C for eight hours.

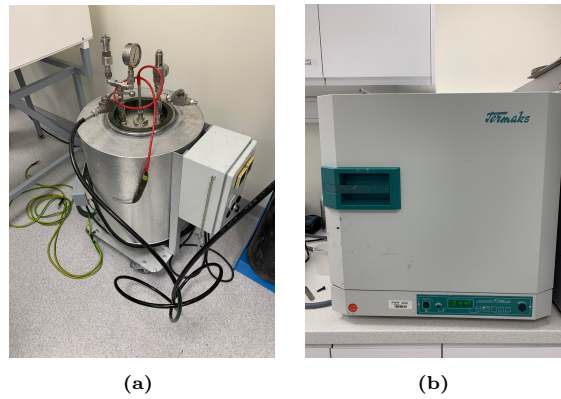


Figure A.10: Curing: (a) Pressure chamber; (b) Heat chamber.

After the curing process, the cups should be hard. Each cup must be inspected under a microscope to uncover cavities or other impurities that could affect its breakdown strength seen in Figure A.11.



Figure A.11: Examination of a cup with a microscope.

B Epoxy with silica filler casting in cup configuration - approach

The same approach in Appendix A is utilized for the epoxy casting with silica flour. However, some adjustments must be made. Due to the addition of silica flour, the viscosity of the fluid increases. Hence the molding time will increase. The mixing is also more complicated as the blending with silica flour is more difficult.

The same flow diagram seen in Figure A.2 is conducted, however, with some adjustments. Steps 1, 2, 5 and 8 presented in Appendix A apply for the epoxy casting with silica flour. The steps that need to be adjusted will be presented here.

3. Measurements

For the measurements, the silica flour is added. It is important to dry the silica flour. This was done in a vacuum for a couple of days before the first casting.

Table B.1: Product data and the mixture relation for one epoxy with silica flour cup portion.

Material	Product name	Quantity [pbw]
Liquid, low viscous bisphenol A epoxy resin	Araldite CY228-1	100
Liquid anhydride hardener	Aradur HY 918-1	85
Solvent-free, low viscous polyglycol	Flexibilizer DY 067	17
Liquid tertiary amine accelerator	Accelerator DY 062	0.6
Filler	Silica flour FW 61 EST	350

From this, the wt. % of the silica flour is calculated to be 65 %.

4. Making set up for casting

Due to the high viscosity of the fluid, an 8 mm tube is used for the setup, compared to the 6 mm tube in Appendix A. A 6 mm tube is connected to the end of the 8 mm tube as this tube is too large to fit the molding holes in the cups. Furthermore, the same setup is used as described in Appendix A.



Figure B.1: Setup for the casting of epoxy with silica cup.

6. Mixing

When mixing, the accelerator is not put into the mixture immediately. This is due to its task of curing the mix at once. Therefore, the epoxy, hardener, flexibilizer and silica flour are first mixed in a vacuum for an hour. After that, the accelerator is out in the mixture, and the mixture is mixed for two hours.

Ultrasound is used for the first mixing, as seen in Figure B.2. When the mixture is nicely mixed, seen in Figure B.2 (c), it is set in the vacuum casting chamber for further mixing.

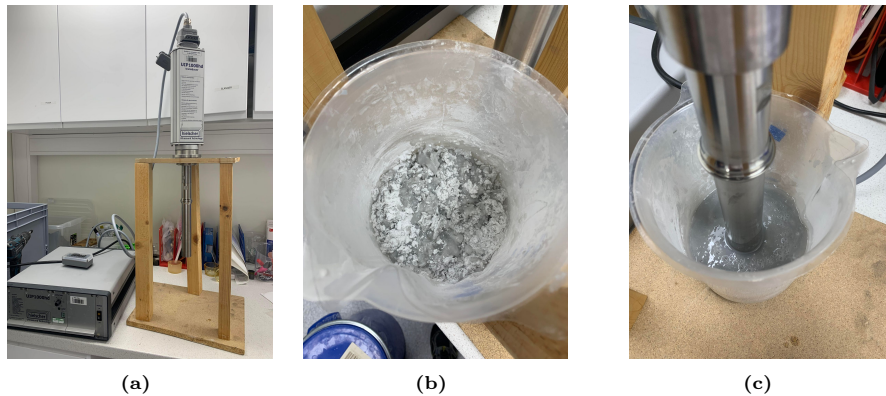


Figure B.2: Mixing: (a) Ultrasound set up; (b) Unmixed (c) Mixed.

7. Molding

One cup is molded at a time, seen in Figure B.1. This is due to the high viscosity of the fluid.

C Examination of test objects before testing

An overview of the cups produced in the casting and the examination of them will now be presented.

The cups are numbered based on the cup and casting number. The cup number is given digit numbering, while the casting number is given letter numbering. An example is cup 2A which is the the second cup made

in the first casting. Further are the cups divided into epoxy cups and epoxy with silica cups.

C.1 Epoxy cups without silica filler: Casting A

For the first casting, an old hardener and accelerator were used. Their structure was brittle, which led to one of them being broken. Hence, only three cups were in the desired shape. However, some of them had cracks and shrinkage in the walls.

The cups were numbered from 1 to 3 from left to right. They are presented in Figure C.1.

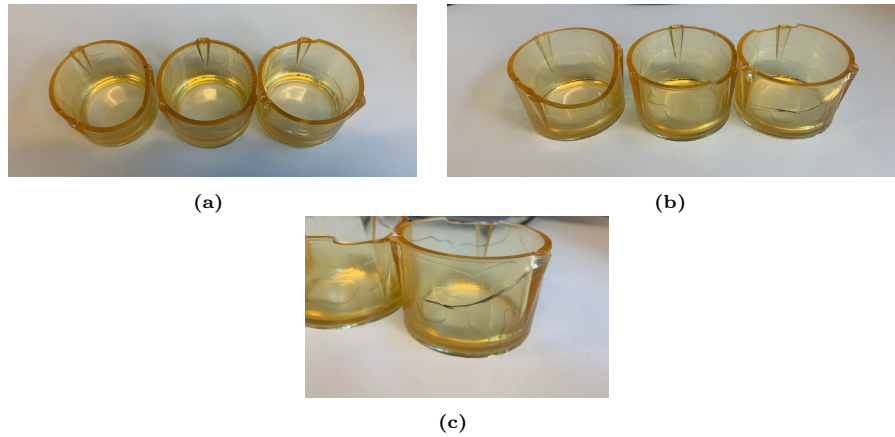


Figure C.1: The epoxy cups made in the first casting: (c) Cup 3A showing a crack in the wall.

The cups were examined under a microscope. Cup 2A is seen in Figure C.2. From Figure C.2 (b), several impurities were spotted. Traces from the casting mold were also observed. No significant difference between cup 2A and the other cups made in this casting was observed with the microscope.



Figure C.2: Cup 2A examined in a microscope: (a) With a magnitude of $\times 20$; (b) With a magnitude of $\times 160$.

Another essential aspect that needs to be addressed is that the cups were not sufficiently taken care of from the moment they were made. They were put into plastic bags after some time. This is a clear source of error regarding the cups produced in this casting.

C.2 Epoxy cups without silica filler: Casting B

A newer hardener and accelerator were used in this casting compared to the casting A. These were also used in the further castings. The cups had a less brittle structure compared to the first casting, making it easier to release the cups from the mold form and less cracks occurred.

The cups seen in Figure C.3 is named 1-4 from left to right.



Figure C.3: The epoxy cups made in the casting B.

Cup 4B in microscope is seen in Figure C.4. It seems that the traces from the molding form decreased compared to the cups produced in the casting A. However, several impurities were spotted during the examinations of the cups.



Figure C.4: Cup 4B examined in a microscope: (a) With a magnitude of x20 ; (b) With a magnitude of x160 .

C.3 Epoxy cups without silica filler: Casting C

The cups in casting C were not in the pressure chamber at 80 °C for 4 hours. This was due to the inertia in the system when putting the timer on for 4 hours. As the pressure in the chamber will help eliminate air bubbles, this situation might have caused air bubbles not to be mitigated.

The cups seen in Figure C.5 is named 1-4 from left to right.

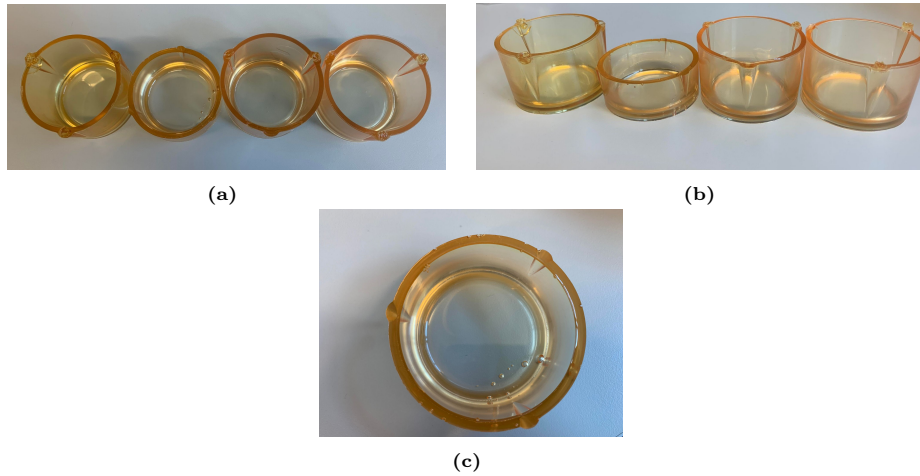


Figure C.5: The epoxy cups made in the third casting: (a) The cups seen from above ; (b) Cup 2C has shorter walls compared to the other cups, due to a leakage; (c) Cup 2C has visible voids .

Cup 1C is presented in Figure C.6



Figure C.6: Cup 1C examined in a microscope: (a) With a magnitude of x20 ; (b) With a magnitude of x160 .

Figure C.7 shows the examinations of cup 2C and 4C. One of the air bubble in cup 2C can be observed in Figure C.7 (a). After examining cup 4C, some bigger impurities compared to the other healthy cups were observed, seen in Figure C.7 (b).

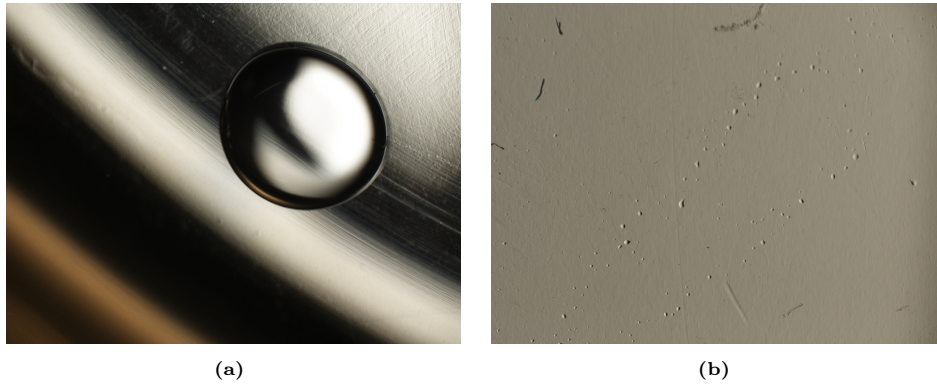


Figure C.7: Cup 2C and 4C examined in a microscope: (a) Cavity at a magnitude of x20 in cup 2C ; (b) Cup 4C at a magnitude of x20.

From the examinations, it can be concluded that cup 2C is not possible to use in further testing due to its short walls and air bubbles.

C.4 Epoxy cups without silica filler: Casting D

For this casting, 6 cups were made. The pressure chamber was too narrow for six. Hence five cups were put in the chamber, while cup number five was set in the heating chamber. Cup number five has shorter walls due to a small leakage.

The cups are numbered from 1 to 6, correlating to the mold form each cup was made in.



Figure C.8: The epoxy cups made in the fourth casting.

When examined under a microscope, no big difference was spotted between the cups. They were much alike the microscope pictures from the casting B and C. No notable variation is seen between each cup in the microscope.

C.5 Epoxy cups with silica filler: Casting A

Five cups were made in this casting process. When put in the pressure chamber, the pressure was forgotten to turn on. Hence air bubbles might not have been mitigated.

The cups are numbered from 1 to 6, correlating to the mold form each cup was made in. Cup 4A have a visible cavity seen in Figure C.9 (c).

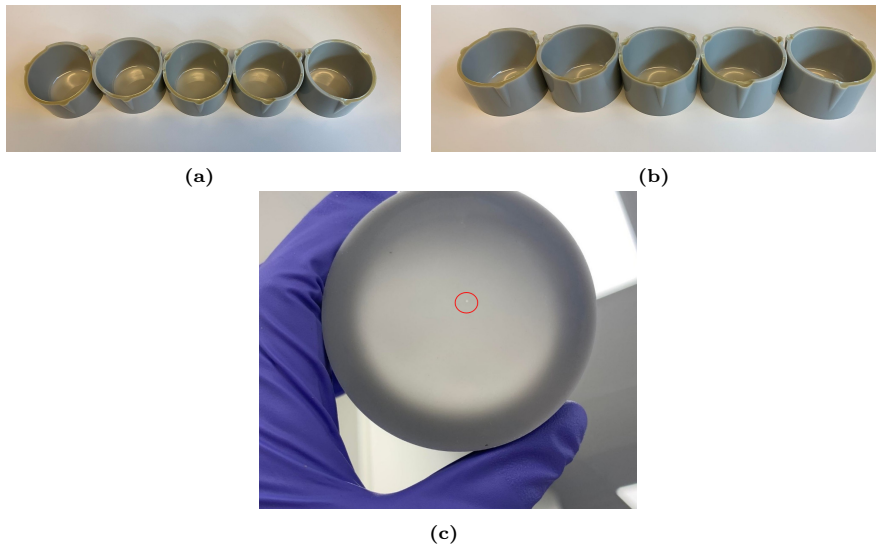


Figure C.9: The cups made in the casting A with silica filler: (c) Cup 4A with red marking around a visible cavity.

As the silica flour makes the cups grey and non-transparent, it is difficult to examine them under a microscope. Hence, visual observation is done to see if any impurities or cavities can be seen. It is essential to be aware that tiny cavities might go under the radar.

All the cups were fine, except for cup number 4, as one cavity was spotted in the middle of the cup. It can therefore be concluded that this cup is not suitable for the testing.

C.6 Epoxy cups with silica filler: Casting B

Four cups were made in the second casting of epoxy with silica flour cups. They are numbered 1-4 from left to right in Figure C.10.



Figure C.10: The epoxy with silica flour cups made in the second casting with silica flour.

By visually inspecting the cups, it can be seen that they are even better than the cups made in the first casting.

